haematologica
Journal of the Ferrata Storti Foundation

Blockade of the CD47/SIRPα checkpoint axis potentiates the macrophage-mediated anti-tumor efficacy of tafasitamab

by Alexander Biedermann, Maria Patra-Kneuer, Dimitrios Mougiakakos, Maike Büttner-Herold, Doris Mangelberger-Eberl, Johannes Berges, Christian Kellner, Sarah Altmeyer, Jörg Thomas Bittenbring, Christian Augsberger, Kristina Ilieva-Babinsky, Stefan Haskamp, Fabian Beier, Christopher Lischer, Julio Vera, Anja Lührmann, Simone Bertz, Simon Völkl, Benedikt Jacobs, Stefan Steidl, Andreas Mackensen, and Heiko Bruns

Received: December 29, 2023.
Accepted: June 19, 2024.

Citation: Alexander Biedermann, Maria Patra-Kneuer, Dimitrios Mougiakakos, Maike Büttner-Herold, Doris Mangelberger-Eberl, Johannes Berges, Christian Kellner, Sarah Altmeyer, Jörg Thomas Bittenbring, Christian Augsberger, Kristina Ilieva-Babinsky, Stefan Haskamp, Fabian Beier, Christopher Lischer, Julio Vera, Anja Lührmann, Simone Bertz, Simon Völkl, Benedikt Jacobs, Stefan Steidl, Andreas Mackensen, and Heiko Bruns. Blockade of the CD47/SIRPa checkpoint axis potentiates the macrophage-mediated anti-tumor efficacy of tafasitamab. Haematologica. 2024 June 27. doi: 10.3324/haematol.2023.284795 [Epub ahead of print]

Blockade of the CD47/SIRPα checkpoint axis potentiates the macrophage-mediated anti-tumor efficacy of tafasitamab.

Alexander Biedermann[1], Maria Patra-Kneuer[2], Dimitrios Mougiakakos[3], Maike Büttner-Herold[4], Doris Mangelberger-Eberl[2], Johannes Berges[1], Christian Kellner[5], Sarah Altmeyer[6], Jörg Thomas Bittenbring[6], Christian Augsberger[2], Kristina Ilieva-Babinsky[2], Stefan Haskamp[7], Fabian Beier[8], Christopher Lischer[9], Julio Vera[9], Anja Lührmann[10], Simone Bertz[11], Simon Völkl[1], Benedikt Jacobs[1], Stefan Steidl[2], Andreas Mackensen[1], and Heiko Bruns[1*]

Affiliations:

[1]Department of Internal Medicine 5, Hematology and Oncology, Friedrich-Alexander-University Erlangen-Nürnberg, Erlangen, Germany.[2] Translational Research, MorphoSys AG, Planegg, Germany. [3]Department of Hematology and Oncology, Otto-von-Guericke University (OVGU) Magdeburg, Magdeburg, Germany. [4]Department of Nephropathology, Institute of Pathology, Friedrich-Alexander-University Erlangen-Nürnberg (FAU), Erlangen, Germany. [5]Division of Transfusion Medicine, Cell Therapeutics and Haemostaseology, University Hospital, LMU Munich, Germany. [6]Medizinische Klinik I, Saarland University Medical School, Homburg/Saar, Germany. [7]Institute of Human Genetics, University Hospital Erlangen, Friedrich-Alexander-University Erlangen-Nürnberg, Erlangen, Germany. [8]Department of Oncology, Hematology and Stem Cell Transplantation, RWTH Medical School, Aachen, Germany. [9]Department of Dermatology, University Hospital Erlangen, Erlangen, GER. [10] Mikrobiologisches Institut, Universitätsklinikum Erlangen, Friedrich-Alexander-Universität Erlangen-Nürnberg, Erlangen, Germany. [11]Institute of Pathology, Universitätsklinikum Erlangen, Friedrich-Alexander-Universität Erlangen-Nürnberg (FAU), Germany

[*]Corresponding author: Heiko Bruns, Dept. of Internal Medicine 5, Hematology and Oncology, Friedrich-Alexander-University Erlangen-Nürnberg (FAU), Erlangen, Germany,

Ulmenweg 18, D-91054 Erlangen. Phone: +49-9131-85-43163, Fax: +49-9131-85-36521, E-Mail: heiko.bruns@uk-erlangen.de

Data availability statement

The original contributions presented in the study are included in the article/Supplementary Material. Further inquiries can be directed to the corresponding author.

Authorship Contributions

A.B. designed and performed experiments and helped write the manuscript. M.P.-K. conceived project, designed experiments and helped write the manuscript. D.M. conceived project, designed the experiments, and helped write the manuscript. M.B.-H., S.B. selected and evaluated histopathological lymphoma specimens and controls and established the immunohistochemical staining. D.M.-E. designed and supervised animal experiments. J.B. designed and performed experiments. C.K., A.L. contributed essential reagents/analytical tools and scientific input. C.A. designed experiments. K.I.-B. designed experiments and helped write the manuscript. S.H., C.L., J.V. performed statistical analysis. S.A., J.B., S.V., F.B., B.J. provided patient materials and provided critical suggestions and discussions throughout the study. S.S. helped write the manuscript. A.M. provided major intellectual input for the project design and helped write the manuscript. H.B. conceived and directed the project and wrote the manuscript.

Acknowledgements

We would like to acknowledge the excellent assistance of the Core Unit Cell Sorting and Immunomonitoring Erlangen.

Funding

H.B. was supported by Wilhelm-Sander Foundation, by the Research Training Group 2740 “Immunomicrotope” (project B3), by German Cancer Foundation (Grant no. 70114489) and

by the SFB TR 221 (project B12). M.B.-H. was supported by the SFB TR 221 (project Z01). A.L. was supported by the Research Training Group 2740 “Immunomicrotope” (project A3).

Conflicts of interest

M. PK., D.ME, C.A., K. IB. and S.S. are employees of Morphosys AG. S.S. owns MorphoSys stocks. M.P. and S.S. hold MorphoSys patents. This study received funding from MorphoSys AG. The funder was involved in study design, collection, analysis, interpretation of the data, writing of this article and decision to submit it for publication.

Abstract

Macrophages are one of the key mediators of the therapeutic effects exerted by monoclonal antibodies, such as the anti-CD19 antibody tafasitamab, approved in combination with lenalidomide for the treatment of relapsed or refractory (r/r) diffuse large B cell lymphoma (DLBCL). However, antibody-dependent cellular phagocytosis (ADCP) in the tumor microenvironment can be counteracted by increased expression of the inhibitory receptor SIRPα on macrophages and its ligand, the immune checkpoint molecule CD47 on tumor cells. The aim of this study was to investigate the impact of the CD47-SIRPα axis on tafasitamab-mediated phagocytosis and explore the potential of anti-CD47 blockade to enhance its anti-tumor activity. Elevated expression of both SIRPα and CD47 was observed in DLBCL patient-derived lymph node biopsies compared to healthy controls. CRISPR-mediated CD47 overexpression impacted tafasitamab-mediated ADCP *in vitro* and increased expression of SIRPα on macrophages correlated with decreased ADCP activity of tafasitamab against DLBCL cell lines. Combination of tafasitamab and an anti-CD47 blocking antibody enhanced ADCP activity of *in vitro* generated macrophages. Importantly, tafasitamab-mediated phagocytosis was elevated in combination with CD47 blockade using primary DLBCL cells and patient-derived lymphoma-associated macrophages (LAMs) in an autologous setting. Furthermore, lymphoma cells with low CD19 expression were efficiently eliminated by the combination treatment. Finally, combined treatment of tafasitamab and an anti-CD47 antibody resulted in enhanced tumor volume reduction and survival benefit in lymphoma xenograft mouse models. These findings provide evidence that CD47 blockade can enhance the phagocytic potential of tumor targeting immunotherapies such as tafasitamab and suggest there is value in exploring the combination in the clinic.

Introduction

Diffuse large B-cell lymphoma (DLBCL) is the most common type of non-Hodgkin lymphoma[1]. Approximately 60-70% of newly diagnosed DLBCL patients can be cured using first-line standard of care - a combination of the anti-CD20 antibody rituximab and cyclophosphamide, doxorubicin, vincristine, and prednisone (R-CHOP). The remaining 30-40% of DLBCL patients experience relapse or refractory disease with poor survival rates. This highlights an unmet clinical need for more effective therapies for a substantial subset of patients[2, 3].

Tafasitamab is an Fc-modified, humanized monoclonal anti-CD19 antibody immunotherapy. Tafasitamab received accelerated approval by the FDA (2020) and conditional marketing authorization by the EMA (2021) for the treatment of transplant-ineligible adult patients with relapsed or refractory (r/r) DLBCL in combination with the immunomodulatory drug lenalidomide (LEN). The Fc region of tafasitamab was engineered to bind Fcγ receptors with higher affinity than a wild type counterpart, resulting in enhanced antibody-dependent cell-mediated cytotoxicity (ADCC)[4] and antibody-dependent cellular phagocytosis (ADCP)[5].

Macrophages are critical mediators of antibody therapy in DLBCL and represent one of the key components of the lymphoma microenvironment[6, 7]. However, lymphoma-associated macrophages (LAMs) are often compromised by the tumor microenvironment in executing their effector functions[8-10]. In particular, the checkpoint molecule CD47 has been shown to be highly expressed by various types of B-cell-derived lymphomas. CD47 mediates immune escape from macrophage-mediated phagocytosis upon interaction with phagocyte-expressed signal regulatory protein alpha (SIRPα), a protein expressed by macrophages, granulocytes, and dendritic cells[11]. Furthermore, frequency of SIRPα-expressing LAMs was reported to be increased in patients with follicular lymphoma (FL), who relapse after initial treatment with lenalidomide and rituximab, indicating that macrophages with reduced phagocytic capacity

may influence the outcome of antibody immunotherapy regimens[12]. However, antibody blockade of either CD47 or SIRPα was shown to strongly enhance ADCP by macrophages[10, 13]. Furthermore, a recent report of a phase Ib study suggested there may be promise in the combination of CD47 blockade with rituximab in B-NHL patients[14]. Based on the reported properties of the CD47-SIRPα axis to interfere with innate and antibody-dependent phagocytosis, we hypothesized that combining tafasitamab with a CD47 blocking antibody can increase its ADCP activity and has the potential to improve its efficacy.

Methods

Isolation of LAMs, macrophages or lymphoma cells from human samples

Bone marrow (BM) samples from healthy individuals or DLBCL patients (with pre-confirmed tumor cell infiltration), and lymph node biopsies (single cell suspension) from DLBCL patients (with pre-confirmed tumor cell infiltration) were stained with CD163, CD15 and CD20 antibodies. Macrophages (CD163+/CD15-) and B cells (CD20+) were isolated by fluorescence-activated cell sorting (FACS). Purity was greater than 95%, determined via flow cytometry. All human material was obtained with written informed consent in accordance with the declaration of Helsinki and its use was approved by the institutional ethics committee (Aachen: EK206/09; Erlangen: Ref. number 3555, 36_12 B, 219_14B, 200_12B).

Flow cytometry-based phagocytosis assay

CPD labelled lymphoma cells were co-cultured with macrophages (E:T=5:1) in sterile FACS tubes in the presence or absence of tafasitamab (1µg/ml) and/or anti-CD47 antibody (B6H12, 1µg/ml) for 24 hours in R10 supplemented with heat inactivated FCS (56 °C or for 30 minutes, to inactivate complement). In some experiments, the CD47-IgGσ clone (1µg/ml) was used instead[15]. Target lymphoma cells were stained with CPD and macrophage effector cells

were counterstained with anti-human CD11b-PeCy7 antibody. Absolute numbers of surviving CD11b-/CPD+ lymphoma cells were determined using 123count eBeads (eBioscience). Percentage of antibody mediated phagocytosis was calculated using the following formula: [%] = 100 – ((absolute number of surviving lymphoma cells in the presence of antibody / absolute number of surviving lymphoma cells in absence of antibody) × 100).

Fluorescence microscopy-based phagocytosis assay

Lymphoma cells were stained with Incucyte® Cytolight Rapid Green Dye and co-cultured with macrophages (E:T=1:1) on an 8-chamber slide in the presence or absence of tafasitamab (1µg/ml) and/or anti-CD47 antibody (B6H12, 1µg/ml), for 3 hours. Adherent cells were washed with PBS and stained with anti-human CD11b-APC antibody and subsequently fixed with 4% paraformaldehyde (PFA) in PBS. The slide was overlaid with 4',6-diamidino-2-phenylindole (DAPI) medium and covered with a glass cover slide. Slides were stored in the dark at 4°C. Slides were analyzed in z-stack sections creating up to 10 optical slices (0.5 µm thick each) using a confocal microscope (LSM700, Zeiss) at x630 magnification. To analyse phagocytosis activity, at least five different fields of view per condition and up to 100 macrophages in total were counted in a blinded manner.

Statistical analysis

GraphPad Prism and Microsoft Excel software were used for statistical analyses. Comparisons between patients and controls were performed with nonparametric Mann-Whitney U-test. For *in vitro* experiments, two tailed Students t test was performed pairwise between treatment and control groups or between single and combination treatment groups. Results are presented as mean ± standard error of the mean (SEM). For *in vivo* experiments, survival data was analyzed using logrank (Mantel-Cox) test. Differences were considered significant if $p<0.05$.

Additional methods used in this study are described in the supplemental Methods, available on the Haematologica website.

Results

Increased expression of CD47 and SIRPα in DLBCL

Interaction of CD47 with SIRPα triggers a "don't eat me" signal in macrophages, inhibiting efficient ADCP. To investigate whether the CD47-SIRPα axis is altered in DLBCL patients, we performed multiplex immunostaining including CD47, CD19, CD68 (pan-macrophage marker), and SIRPα in DLBCL specimens (n=9) or healthy controls (n=7) (for patient characteristics see Supplemental table 1 and Supplemental table 2). In fact, we found strongly enhanced CD47 expression on lymphoma cells compared to healthy donor B-cells (mean value of the DLBCL group: 777±135 MFI vs. mean value of the control group: 277±58 MFI; $p<0.0001$) (**Figure 1A and Supplemental Figure 1A**). Moreover, the percentage of $CD47^+$ B cells in DLBCL specimens was also significantly increased compared to healthy donors (**Supplemental Figure 1C**). Simultaneously, SIRPα levels were significantly elevated on LAMs of DLBCL patients (mean value of the DLBCL group: 1824±462 MFI vs. mean value of the control group: 627±102 MFI; $p<0.0001$) in comparison to healthy donor macrophages (**Figure 1B and Supplemental Figure 1B**). To determine whether this observation is limited to the lymph node or also found in the bone marrow (BM) of lymphoma patients, we examined CD47 and SIRPα expression in tumor-infiltrated BM biopsies of DLBCL patients (n=9) using flow cytometry (for patient characteristics see Supplemental table 2) (**Figures 1C and 1D**). Similar to the pattern observed in lymph node samples, BM-infiltrating lymphoma cells displayed significantly increased expression of CD47 compared to B-cells in BM samples from healthy individuals (n=8) (controls: 5977±3530 MFI vs. DLBCL: 12535±3744 MFI, $p = 0.002$) (**Figure 1C**). In addition, LAMs in the BM of DLBCL patients showed an increased expression of SIRPα (controls: 8981±2206 MFI vs. DLBCL: 12856±1781 MFI, $p = 0.001$) in comparison to BM macrophages of healthy controls (**Figure 1D**). Furthermore, we used publicly available transcriptomics data (GSE178965) from lymph node biopsies of newly diagnosed or relapsed DLBCL patients to analyse CD47 and SIRPα expression patterns

(**Supplemental Figure 2**). Transcriptomic analysis revealed that CD47 and SIRPα mRNA expression levels in relapsed patients were similar to those in newly diagnosed patients, suggesting that in both relapsed and newly diseased DLBCL patients, the CD47-SIRPα axis may represent a hurdle to effective antibody therapy.

The CD47-SIRPα axis impairs tafasitamab-mediated phagocytosis

Based on the elevated expression of CD47 and SIRPα in DLBCL, we reasoned that the "don´t eat me" axis could affect tafasitamab-mediated phagocytosis. To test this, we performed a flow cytometric phagocytosis assay[16] using macrophages with variable levels of SIRPα expression as effector cells and different DLBCL cell lines (HT, Toledo, U2946) as target cells. CD19 and CD47 expression were in a similar range on the tested cell lines (**Supplemental Figure 3**). Interestingly, we discovered a significant inverse correlation between the level of SIRPα expression (determined as the SIRPα MFI) and tafasitamab-mediated phagocytosis (HT: coefficient = 0.39, $p = 0.017$; Toledo: coefficient = 0.75, $p < 0.001$; U2946: coefficient = 0.56, $p = 0.002$) (**Figure 2A**), suggesting that a high SIRPα expression on macrophages can attenuate tafasitamab´s phagocytic potential *in vitro*. Next, we examined the effects of differential CD47 expression on tafasitamab-mediated phagocytosis. Using CRISPR/Cas9 genome editing, we generated a CD47 knockout variant ($CD47^{KO}$) and a CD47 overexpressing variant ($CD47^{high}$) from the wild type (WT) cell line Toledo. While CD47 was barely detectable on $CD47^{KO}$ cells by flow cytometry, $CD47^{high}$ cells showed a twofold increase compared to WT (**Figure 2B**). Macrophages were co-incubated with the different variants in the presence or absence of tafasitamab and phagocytosis was measured by flow cytometry. Compared to the wild type cells, the CD47 knockout variant was increasingly phagocytosed by macrophages, whereas the CD47 overexpressing cells were resistant to tafasitamab-mediated phagocytosis (WT: 31±6%; $CD47^{Ko}$: 55±5%; $CD47^{high}$: 7±4%) (**Figure 2C**). To confirm this result, we analyzed tafasitamab-mediated uptake of the

Toledo variants by confocal microscopy. After 3h incubation, tafasitamab induced a nearly complete uptake of all observable $CD47^{KO}$ cells, whereas most $CD47^{high}$ lymphoma cells were not phagocytosed (**Figure 2D and 2E**). Overall, these data suggest that elevated expression of both CD47 on lymphoma cells and SIRPα on macrophages may negatively influence the ADCP activity of tafasitamab.

Blocking CD47 increases tafasitamab-mediated phagocytosis

Next, we aimed to counteract the effects of the CD47-SIRPα-axis by using an anti-CD47 monoclonal antibody (mAb). For this purpose, we analyzed phagocytosis of lymphoma cells upon combined treatment of tafasitamab and an anti-CD47 mAb (clone: B6H12). Using confocal microscopy, we observed that the combination resulted in significantly increased phagocytosis of all tested cell lines, compared to the single treatments (**Supplemental Figure 4, and Figure 3A**). This result was confirmed in flow cytometric phagocytosis assays, demonstrating that combined treatment with tafasitamab and anti-CD47 mAb significantly increased phagocytosis rates (%) of Toledo (tafasitamab: 32±24% vs. tafasitamab + anti-CD47: 72±21%; $p<0.001$), U2946 (tafasitamab: 32±18% vs. tafasitamab + anti-CD47: 72±19%; $p=0.002$), and HT (tafasitamab: 32±17% vs. tafasitamab + anti-CD47: 72±16%; $p<0.001$) cells (**Figure 3B**). Since the previous experiments represent only a snapshot at the time point of 3 hours, we performed real-time Incucyte® analysis to observe phagocytosis over a longer period (**Figure 3C**). Measured over a time span of 6 hours, clearance of lymphoma cells was increased under combined treatment of tafasitamab and anti-CD47 mAb compared to single treatments. Since it cannot be excluded that the anti-CD47 clone (B6H12, mouse IgG1), used in the above experiments, triggers ADCP on its own via engagement of Fc receptors, we used an Fc-modified antibody variant (CD47-IgGσ) with abrogated FcγR binding as a control[15]. Independent of their Fc domain, both CD47 antibodies significantly

increased tafasitamab-mediated phagocytosis of lymphoma cells (**Supplemental Figure 5**), suggesting that enhanced phagocytosis results from blockade of the CD47 signalling pathway. Next, the effect of combination treatment was examined on primary patient samples (for patient characteristics see Supplemental table 2). LAMs were isolated from lymph node (LN) or bone marrow (BM) biopsy samples of DLBCL patients (newly diagnosed) using fluorescence-activated cell sorting and co-cultured with isolated autologous lymphoma cells in the presence or absence of tafasitamab ± anti-CD47 mAb (**Figure 4A and Figure 4B**). LAMs isolated from LN or BM samples showed similar tafasitamab-mediated phagocytosis efficiency to *in vitro* differentiated macrophages. Furthermore, combination treatment of tafasitamab and anti-CD47 resulted in significantly increased phagocytosis of autologous lymphoma cells *ex vivo*, compared to monotherapy arms (LN, tafasitamab: 40±14% vs. tafasitamab + anti-CD47: 60±12%; p=0.002) (BM, tafasitamab: 41±23% vs. tafasitamab + anti-CD47: 60±28%; p=0.05) (**Figure 4C**). These results suggest that CD47 blockade can improve the phagocytic activity mediated by tafasitamab targeting primary DLBCL patient cells.

Combination of tafasitamab and anti-CD47 enhances phagocytosis of CD19-low lymphoma cells.

CD19 expression in lymphoma is characterised with high variability and diminished CD19 expression was observed in a substantial percentage of DLBCL patients (24% to 33%) in different studies[17, 18]. Thus, we aimed to determine whether CD47 blockade can boost the phagocytic potential of tafasitamab against lymphoma cells with low CD19 expression. To simulate this scenario, we sorted Toledo cells based on their CD19 expression level into a high (CD19high) and low CD19 (CD19low) population (CD19low with four times lower MFI than CD19high cells) (**Figure 5A and Supplemental Figure 6A**) and co-incubated them with

macrophages in the presence or absence of tafasitamab, anti-CD47 or the combination of both. Notably, isolated lymphoma cells showed no significant difference in terms of viability or CD47 expression **(Supplemental Figure 6B)** and the difference in CD19 expression was stable for 24h after sorting. As expected, tafasitamab-mediated phagocytosis of CD19low cells was decreased compared with phagocytosis of CD19high target cells (CD19high: 41±7% vs. CD19low: 15±9%) (**Figure 5B**). Treatment with anti-CD47 alone mediated a similar increase in phagocytosis in both CD19low- and high-expressing lymphoma cells compared to control samples. Most importantly, combination treatment compared to tafasitamab alone significantly increased phagocytosis of CD19low cells, which was in a similar range as the phagocytosis rate of CD19high cells (CD19high: 56±7% vs. CD19low: 54±10%). These results could also be verified using confocal microscopy. While ~40% of CD19 high cells were ingested by macrophages upon tafasitamab treatment, only ~10% of CD19low cells were phagocytized (**Figure 5C and Figure 5D**). Consistent with the flow cytometry data, combination treatment of tafasitamab and anti-CD47 induced similar level of increase in phagocytosis of both CD19high and CD19low cells when compared to tafasitamab treatment alone. Taken together, these data suggest that addition of anti-CD47 blockade enhances tafasitamab-mediated phagocytic elimination of lymphoma cells with low CD19 expression.

Combination therapy of tafasitamab and anti-CD47 antibody prolongs animal survival and decelerates tumor growth in mice.

To assess the combination of tafasitamab and an anti-CD47 antibody *in vivo*, we used two different lymphoma xenograft models. First, we used a disseminated Ramos C.B-17 SCID model. SCID mice have functional NK cells mediating ADCC, which is an additional important mode of action of tafasitamab besides ADCP. Ramos cells express high levels of CD47 and CD19 (**Supplemental Figure 7**) and are commonly used to assess the *in vivo*

performance of antibody therapeutics[19, 20]. Between days 5 and 21 post tumor cell inoculation, mice were treated with either vehicle control (PBS), tafasitamab, anti-CD47 antibody (clone B6H12) or the antibody combination (**Figure 6A**). While control-treated mice reached endpoints after a median of 25 days, treatment with tafasitamab or anti-CD47 alone showed significantly improved outcomes with a median survival of 35 days or >99 days, respectively (**Figure 6B**: tafasitamab vs. control: $p < 0.0001$, anti-CD47 vs. control: $p < 0.0001$). Combination treatment yielded significantly improved survival compared to the single treatments, as 0/15 tafasitamab-treated, 11/15 anti-CD47-treated and 15/15 combination-treated mice were alive at the end of the study (tafasitamab vs. tafasitamab + anti-CD47: $p < 0.0001$, anti-CD47 vs. tafasitamab + anti-CD47: $p=0.035$).

Next, the combination was tested in a flank Ramos xenograft model in NOD/SCID mice. In NOD/SCID mice, NK cell function is partially compromised and binding affinity of murine SIRPα to human CD47 is increased compared to SIRPα from other mouse strains or human SIRPα[21-23]. Treatment with either vehicle control (PBS), tafasitamab, anti-CD47 antibody (clone B6H12) or the antibody combination started on day 6 after tumor cell inoculation and continued for up to 4 weeks (**Figure 6C**). While tumor growth delay was observed in the tafasitamab- and anti-CD47- monotherapy groups when compared to the vehicle control (2 or 14 days respectively), the combination outperformed the monotherapies (**Figure 6D**). Percent survival was determined by the number of animals reaching maximal tumor volume of 1500 mm^3 until the end of the study (**Figure 6E**). On day 55, 0/10 control-, 0/10 tafasitamab-treated, 1/10 anti-CD47 antibody-treated animals were still alive, while, 7/10 animals were still alive in the combination treatment group, demonstrating a significant survival benefit of the combination treatment compared to the single treatments (tafasitamab vs. tafasitamab + anti-CD47 mAb: $p < 0.0001$; anti-CD47 vs. tafasitamab + anti-CD47: $p = 0.0017$). In

summary, CD47 checkpoint blockade enhances the anti-tumor efficacy of tafasitamab in lymphoma tumor models *in vivo*.

Discussion

In high grade B-cell lymphomas such as DLBCL, macrophages represent a key component of the tumor microenvironment and significant sentinels of the anti-tumor immune response [24, 25]. Despite the fact that macrophages are important effector cells for antibody-based therapies, lymphoma cells can manipulate the effector functions of macrophages via altered expression of proteins [26-28] and counteract their ADCP capacity via the CD47/SIRPα axis[10]. In this study, we show that expression of CD47 and SIRPα is upregulated in primary DLBCL samples. While the studied patient population in this work was small, a significant increase in CD47 expression was detected in both lymph nodes and tumor-infiltrated bone marrow of DLBCL patients, which is in line with previous studies [29, 30]. It has also been reported that high CD47 mRNA expression is associated with a poorer clinical prognosis in DLBCL, B-chronic lymphocytic leukemia (B-CLL) and mantle cell lymphoma (MCL) and a higher risk of death in DLBCL patients[10, 31]. Moreover, we found that primary human LAMs from DLBCL patients exhibited increased expression of the CD47 interaction partner SIRPα. Interestingly, a correlation of high SIRPα gene expression with a favorable survival patients with R-CHOP treatment was reported for DLBCL [31], while high SIRPα expression on LAMs was reported to correlate with poorer survival in patients with FL[32]. In addition, patients with FL who relapse or progress after frontline lenalidomide and rituximab (R^2) treatment, displayed an increased percentage of SIRPα positive LAMs[12], which may suggest that this is a mechanism of resistance to R^2 in these patients.

It is unclear why LAMs exhibit increased SIRPα expression in comparison to non-malignant controls. While CD47 expression is regulated by the MYC oncogene[33] and cytokines such as IL-4 [34], not much is known about the regulation of SIRPα. However, a recent study showed that SIRPα expression in tumor-associated macrophages is transcriptionally repressed by the cyclin-dependent kinase inhibitor CDKN1A (p21)[35]. Thus, it would be interesting to clarify in

future studies whether p21 or other factors are also responsible for the high SIRPα expression in DLBCL associated LAMs.

Using cell line models, we demonstrated that the CD47/SIRPα axis can negatively impact phagocytic activity mediated by the CD19-targeting antibody tafasitamab. In line with this, phagocytosis was significantly reduced upon overexpression of CD47 in lymphoma cells, suggesting that lymphomas with particularly high CD47 expression may be resistant to tafasitamab-mediated phagocytosis. Furthermore, we found that combining tafasitamab with an anti-CD47 blocking antibody can enhance tafasitamab-mediated phagocytosis using co-cultures of lymphoma cell lines and *in vitro* differentiated macrophages from healthy donors. Notably, an Fc-modified antibody variant with abrogated FcγR binding (CD47-IgGσ), which did not result in notable phagocytosis when applied alone, was also able to increase tafasitamab-mediated phagocytosis indicating that blocking the CD47/SIRPα axis to decrease the CD47 ”don’t eat me” signal is sufficient to achieve a combination benefit together with tafasitamab. The combination of the Fc-silent CD47-IgGσ with rituximab previously also led to enhanced ADCP compared to rituximab alone[15]. Recently, Wang et al. reported that a SIRPα variant fused to an Fc with inactivated effector function (nFD164) in combination with the anti-CD20 antibody rituximab showed a synergistic antitumor effect in a lymphoma xenograft mouse model suggesting a concordant conclusion[36]. A more recent study by Osario et al. however suggests that anti-CD47 antibodies require both blockade of CD47/SIRP axis and engagement of activating FcγR signaling to achieve significant *in vivo* antitumor activity[37]. More important, the findings that the combination of tafasitamab with an Fc-competent anti-CD47 resulted in increased phagocytosis could be confirmed testing primary lymphoma cells and LAMs *ex vivo* in an autologous setting. This observation is of particular importance, as these effector cells represent up to 50% of the total leukocyte content in lymphomas[24, 38] and have the potential to rapidly eradicate lymphoma cells by phagocytosis[9]. Similar combination benefits as seen for the CD19-targeting antibody tafasitamab in

combination with CD47 blockade were observed for the CD20-targeting antibody rituximab in combination with CD47 blockade in experiments with cell lines and macrophages from healthy donors as well as primary lymphoma cells and LAMs[10, 15]. Our study mainly focused on CD47 blockade with a CD47- targeting antibody in the context of macrophages. In recent years, several reports indicated that also other immune cells including T cells and even NK cells might be affected by blocking of the CD47/SIRPα axis[39-42]. As the CD47/SIRPα axis is contributing to bridging the innate and adaptive immunity, it would be interesting to take this interplay into account in future studies with tafasitamab – especially as ADCC is one of its major modes of action. In DLBCL, CD19 loss or downregulation after CD19-directed therapies such as CART19 treatment is observed [43, 44]. Moreover, CD19 expression in lymphoma is characterized with high variability[18]. Here, we show that Toledo cells with low CD19 expression are as efficiently phagocytosed by macrophages as Toledo cells with high CD19 expression through the combination of tafasitamab and anti-CD47. This observation implies that combination therapy targeting CD19 and CD47 could overcome reduced ADCP efficiency of therapies targeting only CD19 in CD19-low expressing cells.

Finally, the combination of tafasitamab and the anti-CD47 clone B6H12 was tested in two different *in vivo* models engrafted with Ramos cells. Our focus here was to reflect different modes of action including not only ADCP, but also ADCC when examining the drug combination benefit of both antibodies in vivo, wherefore SCID mice containing functional NK cells were selected as one model. The NOD/SCID model was performed as second model, allowing good s.c. tumor engraftment, but having some limitations: compromised NK cells, which likely result in underestimation of tafasitamab's ADCC capacity as well as increased binding affinity of NOD murine SIRPα to human CD47 associated with potentially artificially high anti-tumor effects of anti-CD47 molecules compared to other mouse strains [21-23]. Importantly, both approaches yielded significantly improved survival rates of mice compared to the respective mono treatments. In the past, Chao et al. had obtained similar

combination benefits investigating rituximab and an anti-CD47 in both disseminated as well as localized Raji xenograft mouse models[10]. More recently, Dheilly et al. generated a dual-targeting bispecific antibody blocking CD47 and CD19 and reported that treatment with the bispecific antibody anti-CD47/CD19 induced significant tumor regression compared to treatment with either anti-CD47 or anti-CD19 antibodies in a Raji mouse model [45]. In this model, the combination of anti-CD47 and anti-CD19 antibodies resulted in a similar reduction of tumor volume as the bispecific antibody, confirming the potent anti-tumor activity upon combination of CD47 blockade with CD19-targeting. Most recently, a fusion protein of a CD20 antibody with the CD47 binding domain of SIRPα was shown to reduce tumor size and activate both macrophages and NK cells via blockade of the CD47/SIRPα interaction and FcγR engagement in different mouse xenograft tumor models[46]. In summary, numerous approaches combining targeting of B cell surface proteins such as CD19 or CD20 and the CD47/SIRPα axis in different molecule formats are currently under investigation and it remains to be elucidated in the future which antigen and format combination will display the best anti-tumor and lowest side effects in lymphoma treatment[47].

In conclusion, the results presented in this study confirm the relevance of the CD47/SIRPα axis in DLBCL and demonstrate that CD47 blockade with a CD47- targeting antibody enhances the phagocytic and anti-tumor activity of the CD19-targeted antibody tafasitamab *in vitro* and *in vivo*.

Whether combination of tafasitamab with other compounds inhibiting the CD47/SIRPα pathway is beneficial is currently investigated in a respective phase 1/2b trial assessing the safety, tolerability and potential clinical benefits of the CD47-targeting SIRPα fusion protein maplirpacept (TTI-662) in combination with tafasitamab and lenalidomide in R/R DLBCL patients (NCT05626322).

About tafasitamab

Tafasitamab is a humanized Fc-modified cytolytic CD19 targeting monoclonal antibody. In 2010, MorphoSys licensed exclusive worldwide rights to develop and commercialize tafasitamab from Xencor, Inc. Tafasitamab incorporates an XmAb® engineered Fc domain, which mediates B-cell lysis through apoptosis and immune effector mechanism including Antibody-Dependent Cell-Mediated Cytotoxicity (ADCC) and Antibody-Dependent Cellular Phagocytosis (ADCP). MorphoSys and Incyte entered into: (a) in January 2020, a collaboration and licensing agreement to develop and commercialize tafasitamab globally; and (b) in February 2024, an agreement whereby Incyte obtained exclusive rights to develop and commercialize tafasitamab globally. Following accelerated approval by the U.S. Food and Drug Administration in July 2020, Monjuvi® (tafasitamab-cxix) is being commercialized in the United States by Incyte. In Europe, Minjuvi® (tafasitamab) received conditional Marketing Authorization from the European Medicines Agency in August 2021. XmAb® is a registered trademark of Xencor Inc.

References

1. Alaggio R, Amador C, Anagnostopoulos I, et al. The 5th edition of the World Health Organization Classification of Haematolymphoid Tumours: Lymphoid Neoplasms. Leukemia. 2022;36(7):1720-1748.
2. Crump M, Neelapu SS, Farooq U, et al. Outcomes in refractory diffuse large B-cell lymphoma: results from the international SCHOLAR-1 study. Blood. 2017;130(16):1800-1808.
3. Pfreundschuh M, Kuhnt E, Trumper L, et al. CHOP-like chemotherapy with or without rituximab in young patients with good-prognosis diffuse large-B-cell lymphoma: 6-year results of an open-label randomised study of the MabThera International Trial (MInT) Group. Lancet Oncol. 2011;12(11):1013-1022.
4. Her JH, Pretscher D, Patra-Kneuer M, et al. Tafasitamab mediates killing of B-cell non-Hodgkin's lymphoma in combination with gammadelta T cell or allogeneic NK cell therapy. Cancer Immunol Immunother. 2022;71(11):2829-2836.
5. Horton HM, Bernett MJ, Pong E, et al. Potent in vitro and in vivo activity of an Fc-engineered anti-CD19 monoclonal antibody against lymphoma and leukemia. Cancer Res. 2008;68(19):8049-8057.
6. Uchida J, Hamaguchi Y, Oliver JA, et al. The innate mononuclear phagocyte network depletes B lymphocytes through Fc receptor-dependent mechanisms during anti-CD20 antibody immunotherapy. J Exp Med. 2004;199(12):1659-1669.
7. Kridel R, Steidl C, Gascoyne RD. Tumor-associated macrophages in diffuse large B-cell lymphoma. Haematologica. 2015;100(2):143-145.
8. Hermann M, Niemitz C, Marafioti T, Schriever F. Reduced phagocytosis of apoptotic cells in malignant lymphoma. Int J Cancer. 1998;75(5):675-679.
9. Bruns H, Buttner M, Fabri M, et al. Vitamin D-dependent induction of cathelicidin in human macrophages results in cytotoxicity against high-grade B cell lymphoma. Sci Transl Med. 2015;7(282):282ra47.
10. Chao MP, Alizadeh AA, Tang C, et al. Anti-CD47 antibody synergizes with rituximab to promote phagocytosis and eradicate non-Hodgkin lymphoma. Cell. 2010;142(5):699-713.
11. Seiffert M, Cant C, Chen Z, et al. Human signal-regulatory protein is expressed on normal, but not on subsets of leukemic myeloid cells and mediates cellular adhesion involving its counterreceptor CD47. Blood. 1999;94(11):3633-3643.
12. Marques-Piubelli ML, Parra ER, Feng L, et al. SIRPalpha+ macrophages are increased in patients with FL who progress or relapse after frontline lenalidomide and rituximab. Blood Adv. 2022;6(11):3286-3293.
13. Petrova PS, Viller NN, Wong M, et al. TTI-621 (SIRPalphaFc): A CD47-Blocking Innate Immune Checkpoint Inhibitor with Broad Antitumor Activity and Minimal Erythrocyte Binding. Clin Cancer Res. 2017;23(4):1068-1079.
14. Advani R, Flinn I, Popplewell L, et al. CD47 Blockade by Hu5F9-G4 and Rituximab in Non-Hodgkin's Lymphoma. N Engl J Med. 2018;379(18):1711-1721.
15. Zeller T, Lutz S, Munnich IA, et al. Dual checkpoint blockade of CD47 and LILRB1 enhances CD20 antibody-dependent phagocytosis of lymphoma cells by macrophages. Front Immunol. 2022;13:929339.
16. Busch L, Mougiakakos D, Buttner-Herold M, et al. Lenalidomide enhances MOR202-dependent macrophage-mediated effector functions via the vitamin D pathway. Leukemia. 2018;32(11):2445-2458.
17. Schuster SJ, Bishop MR, Tam CS, et al. Tisagenlecleucel in Adult Relapsed or Refractory Diffuse Large B-Cell Lymphoma. N Engl J Med. 2019;380(1):45-56.
18. Yang W, Agrawal N, Patel J, et al. Diminished expression of CD19 in B-cell lymphomas. Cytometry B Clin Cytom. 2005;63(1):28-35.
19. Schliemann C, Palumbo A, Zuberbuhler K, et al. Complete eradication of human B-cell lymphoma xenografts using rituximab in combination with the immunocytokine L19-IL2. Blood. 2009;113(10):2275-2283.

20. Daniel D, Yang B, Lawrence DA, et al. Cooperation of the proapoptotic receptor agonist rhApo2L/TRAIL with the CD20 antibody rituximab against non-Hodgkin lymphoma xenografts. Blood. 2007;110(12):4037-4046.
21. Miao M, Masengere H, Yu G, Shan F. Reevaluation of NOD/SCID Mice as NK Cell-Deficient Models. Biomed Res Int. 2021;2021:8851986.
22. Kwong LS, Brown MH, Barclay AN, Hatherley D. Signal-regulatory protein alpha from the NOD mouse binds human CD47 with an exceptionally high affinity-- implications for engraftment of human cells. Immunology. 2014;143(1):61-67.
23. Iwamoto C, Takenaka K, Urata S, et al. The BALB/c-specific polymorphic SIRPA enhances its affinity for human CD47, inhibiting phagocytosis against human cells to promote xenogeneic engraftment. Exp Hematol. 2014;42(3):163-171.
24. Gentles AJ, Newman AM, Liu CL, et al. The prognostic landscape of genes and infiltrating immune cells across human cancers. Nat Med. 2015;21(8):938-945.
25. Mantovani A, Allavena P, Marchesi F, Garlanda C. Macrophages as tools and targets in cancer therapy. Nat Rev Drug Discov. 2022;21(11):799-820.
26. Dahal LN, Dou L, Hussain K, et al. STING Activation Reverses Lymphoma-Mediated Resistance to Antibody Immunotherapy. Cancer Res. 2017;77(13):3619-3631.
27. Izquierdo E, Vorholt D, Blakemore S, et al. Extracellular vesicles and PD-L1 suppress macrophages, inducing therapy resistance in TP53-deficient B-cell malignancies. Blood. 2022;139(25):3617-3629.
28. Su S, Zhao J, Xing Y, et al. Immune Checkpoint Inhibition Overcomes ADCP-Induced Immunosuppression by Macrophages. Cell. 2018;175(2):442-457.e423.
29. Bouwstra R, He Y, de Boer J, et al. CD47 Expression Defines Efficacy of Rituximab with CHOP in Non-Germinal Center B-cell (Non-GCB) Diffuse Large B-cell Lymphoma Patients (DLBCL), but Not in GCB DLBCL. Cancer Immunol Res. 2019;7(10):1663-1671.
30. Cho J, Yoon SE, Kim SJ, Ko YH, Kim WS. CD47 overexpression is common in intestinal non-GCB type diffuse large B-cell lymphoma and associated with 18q21 gain. Blood Adv. 2022;6(24):6120-6130.
31. Carreras J, Kikuti YY, Miyaoka M, et al. Integrative Statistics, Machine Learning and Artificial Intelligence Neural Network Analysis Correlated CSF1R with the Prognosis of Diffuse Large B-Cell Lymphoma. Hemato. 2021;2(2):182-206.
32. Chen YP, Kim HJ, Wu H, et al. SIRPalpha expression delineates subsets of intratumoral monocyte/macrophages with different functional and prognostic impact in follicular lymphoma. Blood Cancer J. 2019;9(10):84.
33. Casey SC, Tong L, Li Y, et al. MYC regulates the antitumor immune response through CD47 and PD-L1. Science. 2016;352(6282):227-231.
34. Pena-Martinez P, Ramakrishnan R, Hogberg C, Jansson C, Nord DG, Jaras M. Interleukin 4 promotes phagocytosis of murine leukemia cells counteracted by CD47 upregulation. Haematologica. 2022;107(4):816-824.
35. Allouch A, Voisin L, Zhang Y, et al. CDKN1A is a target for phagocytosis-mediated cellular immunotherapy in acute leukemia. Nat Commun. 2022;13(1):6739.
36. Wang Z, Hu N, Wang H, et al. High-affinity decoy protein, nFD164, with an inactive Fc region as a potential therapeutic drug targeting CD47. Biomed Pharmacother. 2023;162:114618.
37. Osorio JC, Smith P, Knorr DA, Ravetch JV. The antitumor activities of anti-CD47 antibodies require Fc-FcgammaR interactions. Cancer Cell. 2023;41(12):2051-2065.
38. Newman AM, Liu CL, Green MR, et al. Robust enumeration of cell subsets from tissue expression profiles. Nat Methods. 2015;12(5):453-457.
39. Liu X, Pu Y, Cron K, et al. CD47 blockade triggers T cell-mediated destruction of immunogenic tumors. Nat Med. 2015;21(10):1209-1215.
40. Nath PR, Gangaplara A, Pal-Nath D, et al. CD47 Expression in Natural Killer Cells Regulates Homeostasis and Modulates Immune Response to Lymphocytic Choriomeningitis Virus. Front Immunol. 2018;9:2985.

41. Deuse T, Hu X, Agbor-Enoh S, et al. The SIRPalpha-CD47 immune checkpoint in NK cells. J Exp Med. 2021;218(3):e20200839.
42. van Duijn A, Van der Burg SH, Scheeren FA. CD47/SIRPalpha axis: bridging innate and adaptive immunity. J Immunother Cancer. 2022;10(7):e004589.
43. Yu H, Sotillo E, Harrington C, et al. Repeated loss of target surface antigen after immunotherapy in primary mediastinal large B cell lymphoma. Am J Hematol. 2017;92(1):E11-E13.
44. Shalabi H, Kraft IL, Wang HW, et al. Sequential loss of tumor surface antigens following chimeric antigen receptor T-cell therapies in diffuse large B-cell lymphoma. Haematologica. 2018;103(5):e215-e218.
45. Dheilly E, Moine V, Broyer L, et al. Selective Blockade of the Ubiquitous Checkpoint Receptor CD47 Is Enabled by Dual-Targeting Bispecific Antibodies. Mol Ther. 2017;25(2):523-533.
46. Yu J, Li S, Chen D, et al. IMM0306, a fusion protein of CD20 mAb with the CD47 binding domain of SIRPalpha, exerts excellent cancer killing efficacy by activating both macrophages and NK cells via blockade of CD47-SIRPalpha interaction and Fc□R engagement by simultaneously binding to CD47 and CD20 of B cells. Leukemia. 2023;37(3):695-698.
47. Yang H, Xun Y, You H. The landscape overview of CD47-based immunotherapy for hematological malignancies. Biomark Res. 2023;11(1):15.

Figure Legends

Figure 1. Increased expression of CD47 and SIRPα in diffuse large B cell lymphoma (DLBCL). (**A**) Expression of CD47 on B-cells (CD19+) was quantified using confocal microscopy on tonsils as benign controls (white circles, white bars) (n=7) or DLBCL specimens (red circles, red bars) (n=9). (**B**) SIRPα on macrophages (CD68+) was quantified using confocal microscopy on tonsils as benign controls (white circles) (n=7) or DLBCL specimens (red circles) (n=9). Regions of Interest (ROI) matching B-cells or macrophages were segmented using Zeiss-software (ZEN 2.6) or the open-source software QuPath (https://qupath.github.io), and the mean fluorescence intensity (MFI) of CD47 or SIRPα was assessed for each ROI. Data of 25 cells of each donor were plotted for CD47 or SIRPα. Lines show the mean value. (**C-D**) Bone marrow (BM) biopsies of healthy controls (n=8, white circles) or DLBCL patients with tumor infiltration (n=9, red circles) were analyzed for (**C**) the expression of CD47 on B-cells/lymphoma cells (CD19+/CD20+) or (**D**) SIRPα on macrophages/LAMs (CD163+/CD15-). The graphs (**C-D**) show the result of five independent experiments. Each dot represents a tested donor. Nonparametric Mann-Whitney U-test was performed. Lines show the mean value.

Figure 2. The CD47-SIRPα axis impairs tafasitamab-mediated phagocytosis. (**A**) *In vitro* differentiated macrophages were analyzed for SIRPα expression by flow cytometry before they were used for ADCP assays (n=13). Tafasitamab-induced phagocytosis of HT, Toledo and U2946 cell lines was correlated with SIRPα expression on macrophages. A simple linear model was fitted to the data and the R^2 value was calculated. (**B**) The CRISPR/Cas9 system was used for altering gene expression in Toledo cells. CD47 expression on CD47 knock out ($CD47^{KO}$, light grey), CD47 overexpression ($CD47^{high}$, red) and wild type Toledo (control, dark grey) cells, determined by flow cytometry (n=5). The dotted line represents the

isotype control. MFI is defined as median fluorescence intensity. The bar chart shows average MFI values of three independent measurements. Error bars show SEM. Two tailed paired Students t test was performed. (**C**) Tafasitamab-mediated phagocytosis of control, $CD47^{KO}$ or $CD47^{high}$ cells measured by flow cytometry. Lines show the mean value. The graph shows the result of five independent experiments. Two tailed paired Students t test was performed. (**D**) Immunofluorescence of *in vitro* differentiated macrophages co-cultivated with different cell lines (control, $CD47^{KO}$, $CD47^{high}$) and tafasitamab (1µg/ml) for three hours. Lymphoma cells lines were stained with Cytolight Rapid Green Dye (green), macrophages were stained with CD11b-APC (red). The microscopy images show representative sections of five experiments. (**E**) Quantification of phagocytosis of Toledo cells (control, dark grey) and the genetically modified cells ($CD47^{KO}$: light grey; $CD47^{high}$: red) by confocal microscopy. 100 macrophages per condition were counted and the percentage with ingested lymphoma cells was calculated. The graph shows the result of five independent experiments. Two tailed paired Students t test was performed. Lines show the mean value. Scale bar: 20µm.

Figure 3. Blocking CD47 increases tafasitamab-mediated phagocytosis

(**A**) For quantification of phagocytosis of different DLBCL cell lines (Toledo, U2946, HT) by confocal microscopy, 100 macrophages per condition were counted and the percentage with ingested lymphoma cells was calculated. Lines show the mean value. The graph shows the result of five independent experiments. Two tailed paired Students t test was performed. (**B**) Percentage phagocytosis of lymphoma cell lines using *in vitro* differentiated macrophages as effector cells, in the presence/absence of tafasitamab and anti-CD47-mAb. Phagocytosis was measured with flow cytometry. The diagrams show the results of several independent experiments (Toledo: n=11; U2946: n=23; HT: n=12). Two tailed paired Students t test was performed. Lines show the mean value. (**C**) Phagocytosis of lymphoma cell lines in presence/absence of tafasitamab and/or anti-CD47-mAb for six hours. Incubation and

measurements were performed in absence (white circles) or presence of tafasitamab (dark grey circles) or anti-CD47 (light grey circles) or a combination of both (red circles). Measurements and analysis were conducted using an Incucyte® Live Cell Imaging system microscopy and Incucyte® 2022A software. Total red signal per image was evaluated for all conditions and time points. The course of total red signal is shown in the plots for three cell lines. The graph shows a representative result of three independent experiments.

Figure 4. Blockade of CD47 enhances tafasitamab-mediated phagocytosis of lymphoma-associated macrophages (LAMs).

(**A**) Schematic illustration of flow cytometric isolation of lymphoma-associated macrophages (LAMs) and primary lymphoma cells from bone marrow (n=11) and lymph nodes (n=6) of DLBCL patients. Schematic was created using BioRender.com. (**B**) Representative gating strategy and FACS plots for phagocytosis determination: Isolated lymphoma cells were stained with CPD and co-cultured with isolated LAMs (gate R1). Macrophage effector cells were counterstained with an anti-CD11b antibody and absolute numbers of remaining CD11b-/CPD+ lymphoma cells were determined using counting beads (gate R2). (**C**) Phagocytosis of primary lymphoma cells by LAMs isolated from DLBCL patient bone marrow (BM, left graph) or lymph node (LN, right graph) samples, in the presence/absence of tafasitamab and anti-CD47 mAb. Phagocytosis was measured with flow cytometry. The graphs show the results of several independent experiments (LAMs BM: n=11; LAMs LN: n=6). Two tailed paired Students t test was performed. Lines show the mean value.

Figure 5. Combination of tafasitamab and anti-CD47 increases the elimination of CD19 low-expressing lymphoma cells. (**A**) CD19low (blue histogram) or CD19high (red histogram) Toledo cells were isolated by flow cytometric cell sorting. (**B and C**) Sorted cell populations were immediately incubated with *in vitro* differentiated macrophages and

phagocytosis in the presence or absence of tafasitamab and/or anti-CD47 was determined after three hours by (**B**) flow cytometry or (**C**) confocal microscopy. The diagrams (**B**) summarize the results of 8 macrophage donors tested by FACS in 8 independent experiments. Two tailed paired Students t test was performed. Lines show the mean value. (**C**) CD19low and CD19high Toledo cells were stained with Cytolight Rapid Green Dye (green), macrophages were stained with CD11b-APC (red) and phagocytosis was analyzed by confocal microscopy. Images were taken after washing steps, removing non-adherent and/or non-phagocytosed cells. The microscopy images show representative sections of five performed experiments. Scale bar: 20µm. (**D**) For quantification of phagocytosis of sorted CD19low (upper panel) or CD19high (lower panel) Toledo cells by confocal microscopy, 100 macrophages per condition were counted and the percentage with ingested lymphoma cells was calculated. The graph shows the result of five independent experiments. Two tailed paired Students t test was performed. Lines show the mean value.

Figure 6. Combination treatment of tafasitamab and anti-CD47 antibody prolongs animal survival and decelerates tumor growth in mice. (**A**) Schematic illustration of the disseminated xenograft model. Ramos cells were injected intravenously on D0. Treatment with tafasitamab, anti-CD47 (clone B6H12) and the combination commenced on D5 until D21, followed by continuous monitoring of animals for signs of morbidity until D99. (**B**) Kaplan–Meier plot of the disseminated survival model following treatment with tafasitamab, CD47 mAb or the combination. Tafasitamab vs. control: $p < 0.0001$, anti-CD47 vs. control: $p < 0.0001$, tafasitamab vs. tafasitamab + anti-CD47: $p < 0.0001$, anti-CD47 vs. tafasitamab + anti-CD47: $p = 0.035$ (**C**) Schematic illustration of the flank xenograft model. Ramos cells were injected subcutaneously in the right flank of each mouse on D0. Treatment with tafasitamab, anti□CD47 (clone B6H12) mAb was started and continued for up to 4 weeks and study termination was on day 55. (**D**) Spider plots showing tumor growth curves for

individual animals (n=15) for each treatment group. (**E**) Kaplan–Meier plot showing animal survival until a final tumor volume of 1500 mm^3 was reached. Tafasitamab vs. control: 0.0095, anti-CD47 vs. control: $p < 0.0001$, tafasitamab vs. tafasitamab + anti-CD47 mAb: $p < 0.0001$; anti-CD47 vs. tafasitamab + anti-CD47: $p = 0.0017$

Figure 1

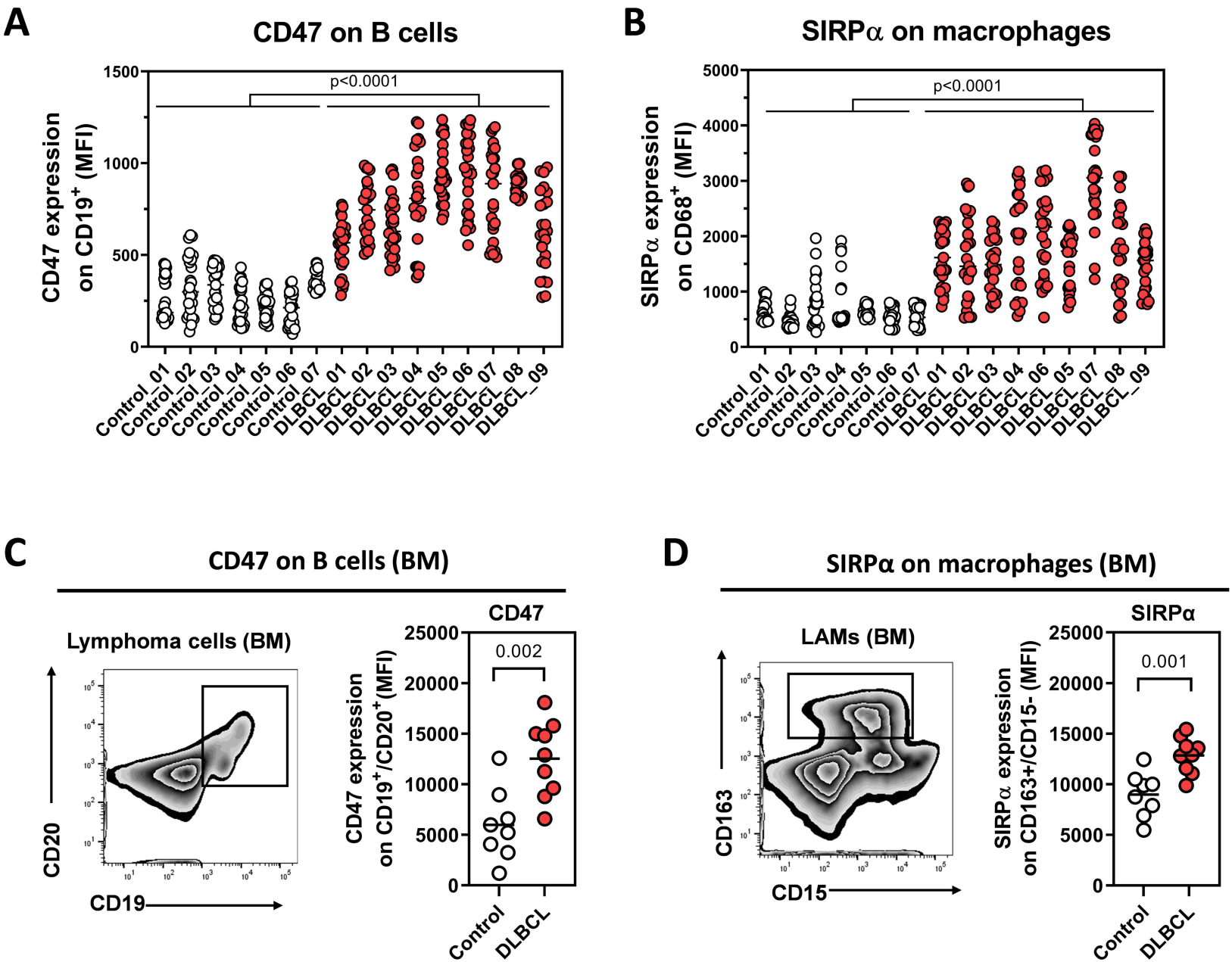
A
CD47 on B cells
CD47 expression on CD19+ (MFI)
p<0.0001
Control_01
Control_02
Control_03
Control_04
Control_05
Control_06
Control_07
DLBCL_01
DLBCL_02
DLBCL_03
DLBCL_04
DLBCL_05
DLBCL_06
DLBCL_07
DLBCL_08
DLBCL_09
B
SIRPα on macrophages
SIRPα expression on CD68+ (MFI)
p<0.0001
C
CD47 on B cells (BM)
Lymphoma cells (BM)
CD20
CD19
CD47
CD47 expression on CD19+/CD20+(MFI)
0.002
Control
DLBCL
D
SIRPα on macrophages (BM)
LAMs (BM)
CD163
CD15
SIRPα
SIRPα expression on CD163+/CD15- (MFI)
0.001
Control
DLBCL

Figure 2

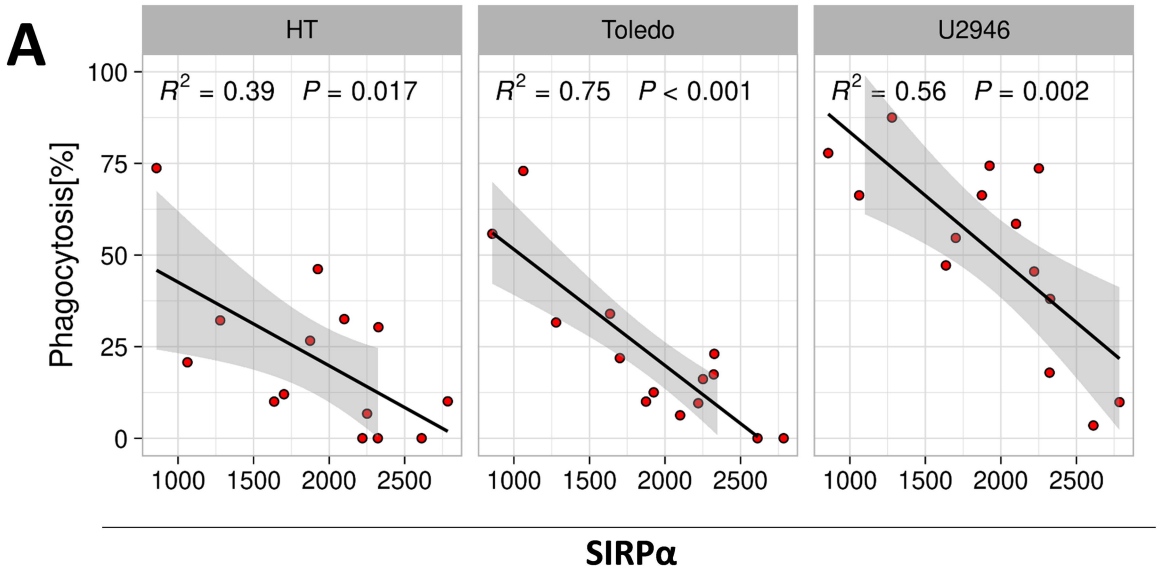
A
HT
Toledo
U2946
R^2 = 0.39 P = 0.017
R^2 = 0.75 P < 0.001
R^2 = 0.56 P = 0.002
Phagocytosis[%]
100
75
50
25
0
1000 1500 2000 2500
SIRPα

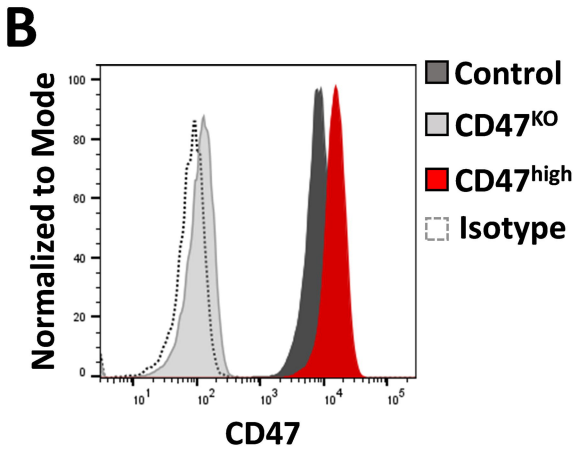
B
Normalized to Mode
CD47
Control
CD47KO
CD47high
Isotype

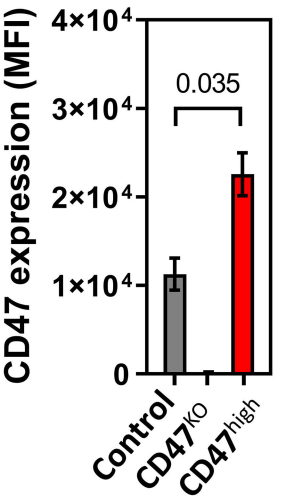
CD47 expression (MFI)
4×10⁴
3×10⁴
2×10⁴
1×10⁴
0
0.035
Control
CD47KO
CD47high

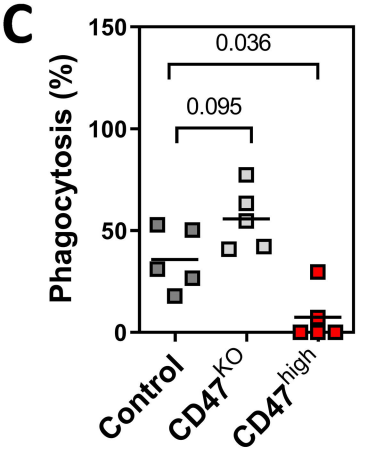
C
Phagocytosis (%)
150
100
50
0
0.036
0.095
Control
CD47KO
CD47high

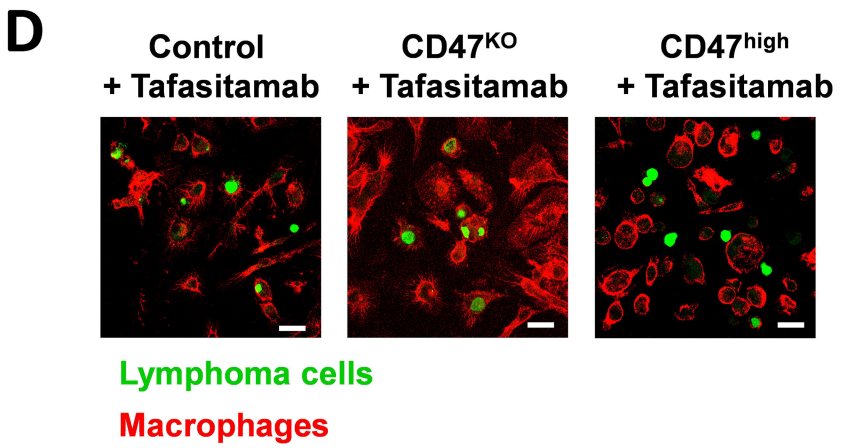
D
Control
+ Tafasitamab
CD47KO
+ Tafasitamab
CD47high
+ Tafasitamab
Lymphoma cells
Macrophages

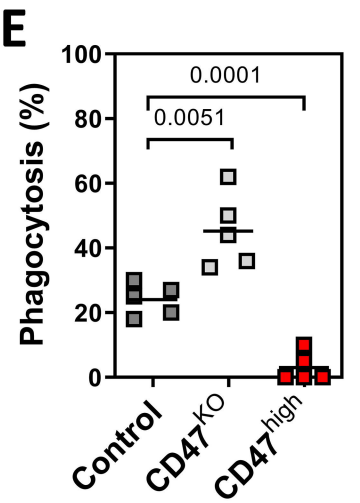
E
Phagocytosis (%)
100
80
60
40
20
0
0.0001
0.0051
Control
CD47KO
CD47high

Figure 3

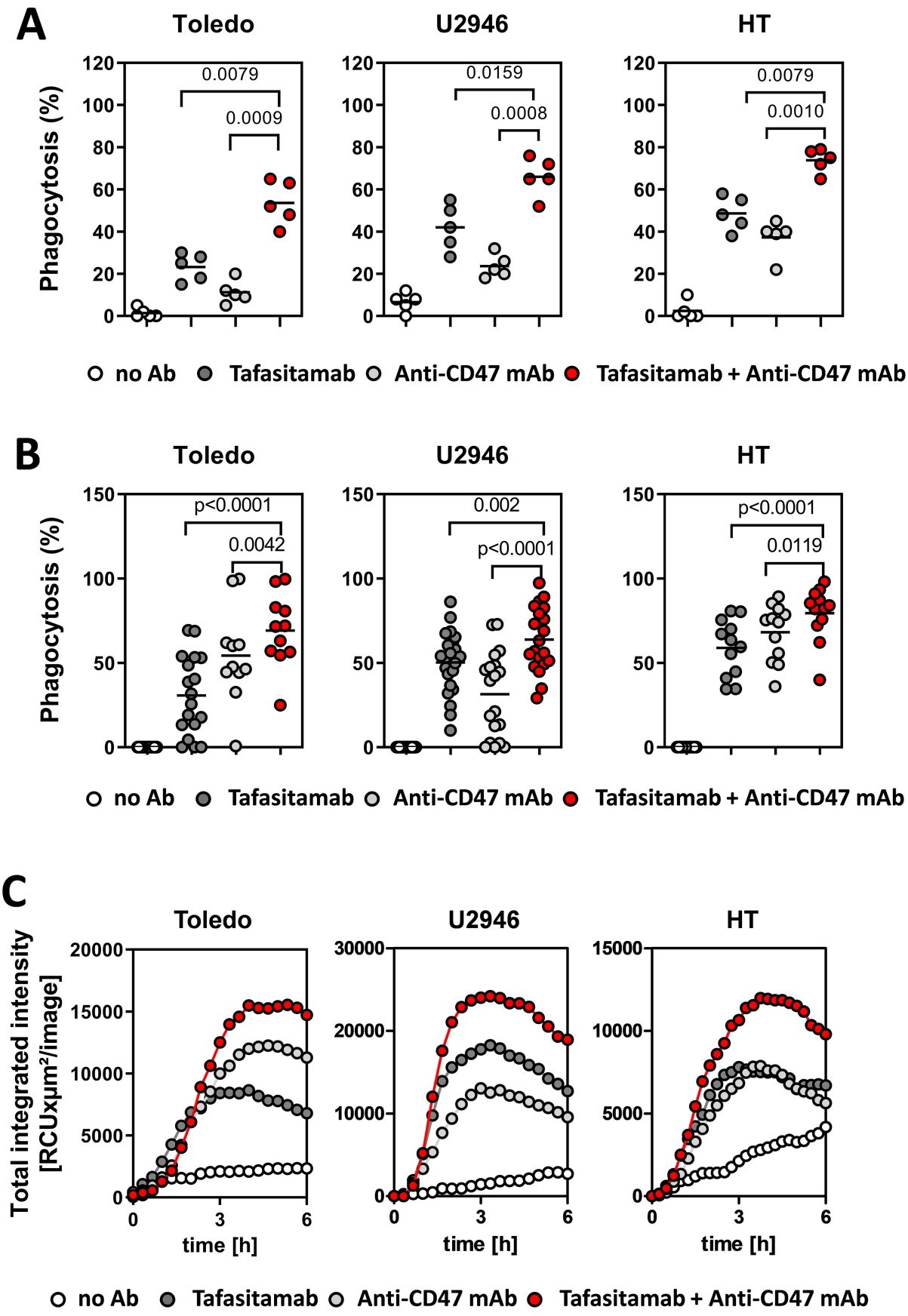
A
Toledo
U2946
HT
Phagocytosis (%)
0.0079
0.0009
0.0159
0.0008
0.0079
0.0010
no Ab
Tafasitamab
Anti-CD47 mAb
Tafasitamab + Anti-CD47 mAb
B
Toledo
U2946
HT
Phagocytosis (%)
p<0.0001
0.0042
0.002
p<0.0001
p<0.0001
0.0119
no Ab
Tafasitamab
Anti-CD47 mAb
Tafasitamab + Anti-CD47 mAb
C
Toledo
U2946
HT
Total integrated intensity [RCUxμm²/image]
time [h]
no Ab
Tafasitamab
Anti-CD47 mAb
Tafasitamab + Anti-CD47 mAb

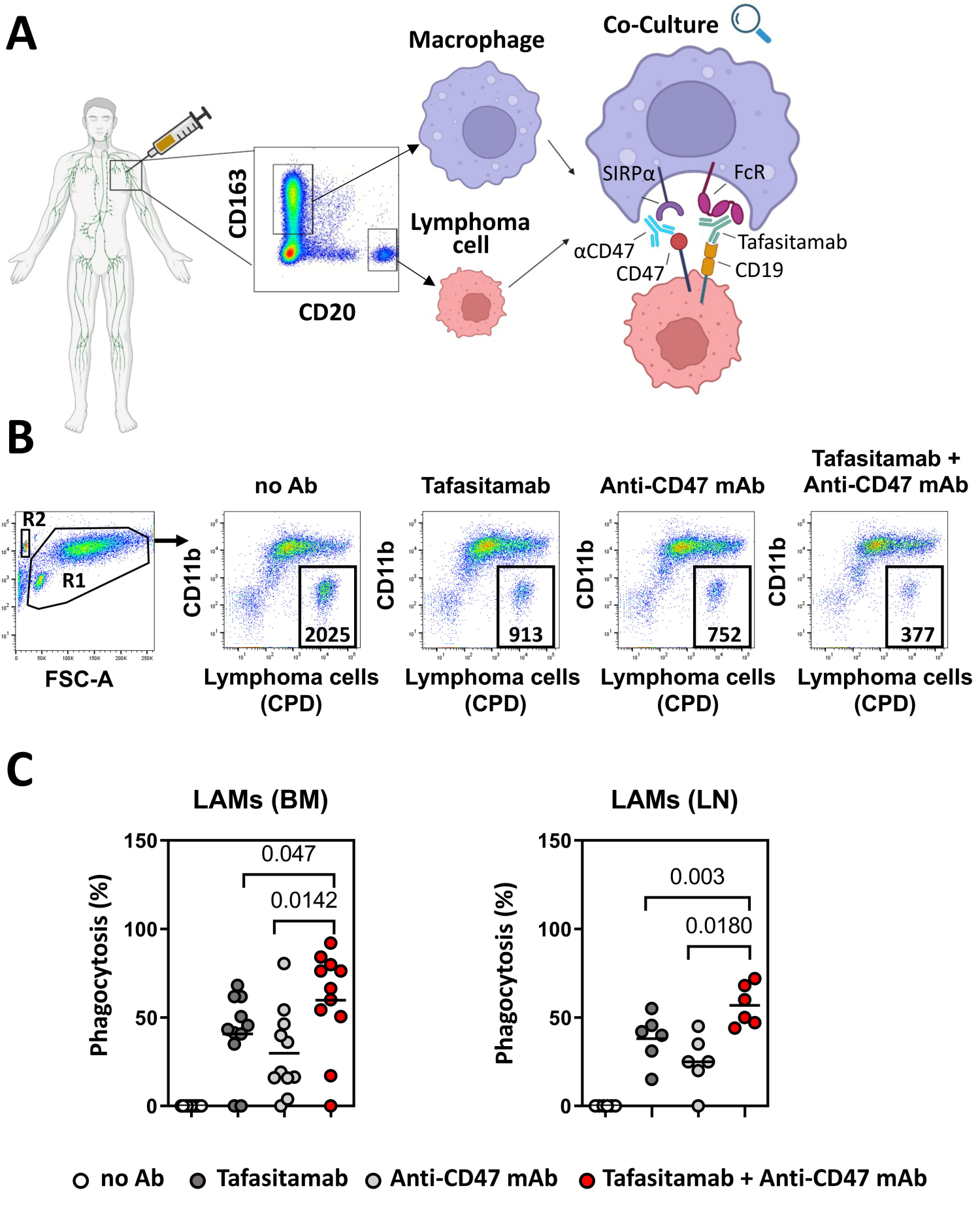
A
Macrophage
Co-Culture
CD163
CD20
Lymphoma cell
SIRPα
FcR
αCD47
CD47
Tafasitamab
CD19
B
no Ab
Tafasitamab
Anti-CD47 mAb
Tafasitamab + Anti-CD47 mAb
R2
R1
SSC-A
FSC-A
CD11b
2025
913
752
377
Lymphoma cells (CPD)
C
LAMs (BM)
LAMs (LN)
Phagocytosis (%)
150
100
50
0
0.047
0.0142
0.003
0.0180
no Ab
Tafasitamab
Anti-CD47 mAb
Tafasitamab + Anti-CD47 mAb

Figure 5

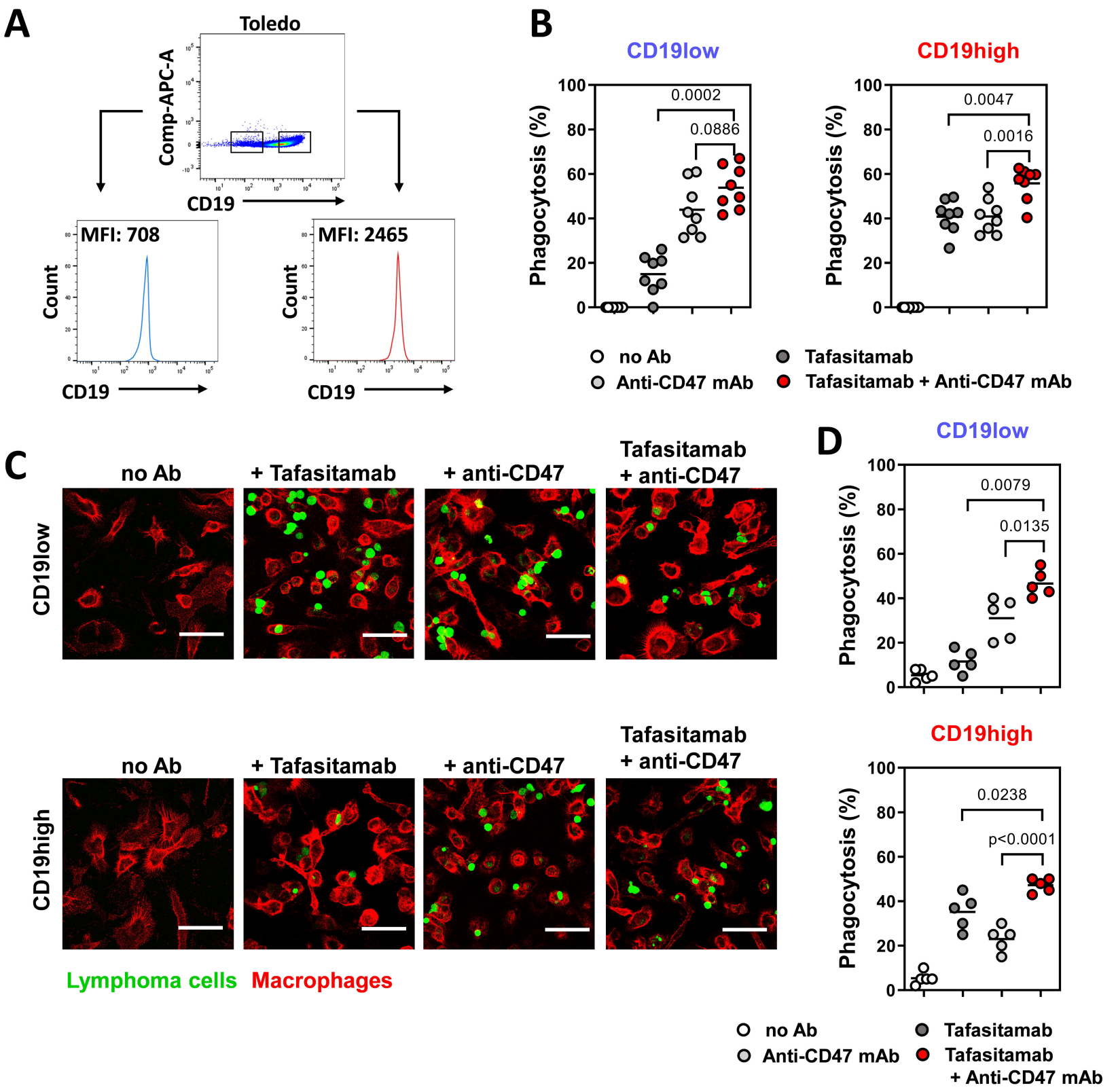
A
Toledo
Comp-APC-A
CD19
MFI: 708
MFI: 2465
Count
CD19
B
CD19low
CD19high
Phagocytosis (%)
0.0002
0.0886
0.0047
0.0016
no Ab
Anti-CD47 mAb
Tafasitamab
Tafasitamab + Anti-CD47 mAb
C
no Ab
+ Tafasitamab
+ anti-CD47
Tafasitamab + anti-CD47
CD19low
CD19high
Lymphoma cells
Macrophages
D
CD19low
CD19high
Phagocytosis (%)
0.0079
0.0135
0.0238
p<0.0001
no Ab
Anti-CD47 mAb
Tafasitamab
Tafasitamab + Anti-CD47 mAb

Figure 6

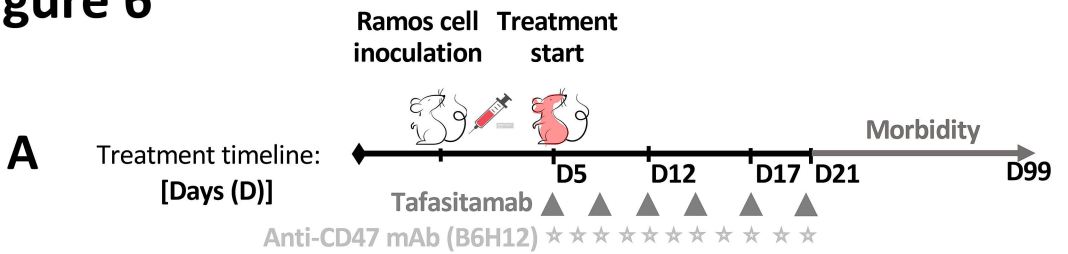
A
Ramos cell inoculation
Treatment start
Treatment timeline:
[Days (D)]
Morbidity
D5
D12
D17
D21
D99
Tafasitamab
Anti-CD47 mAb (B6H12)

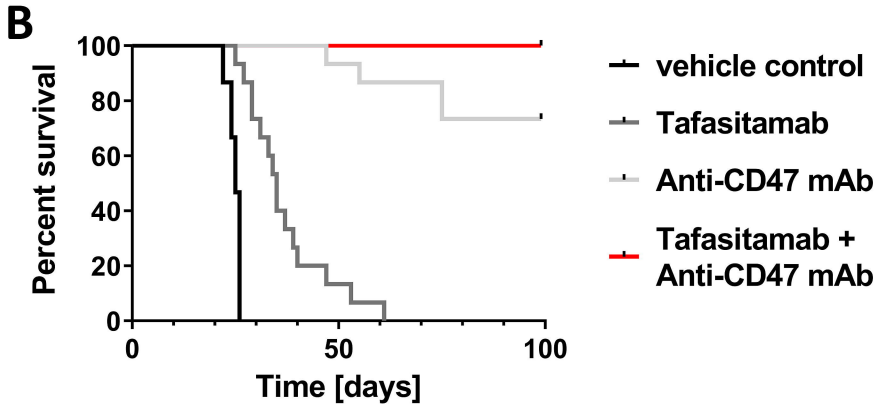
B
Percent survival
Time [days]
vehicle control
Tafasitamab
Anti-CD47 mAb
Tafasitamab + Anti-CD47 mAb

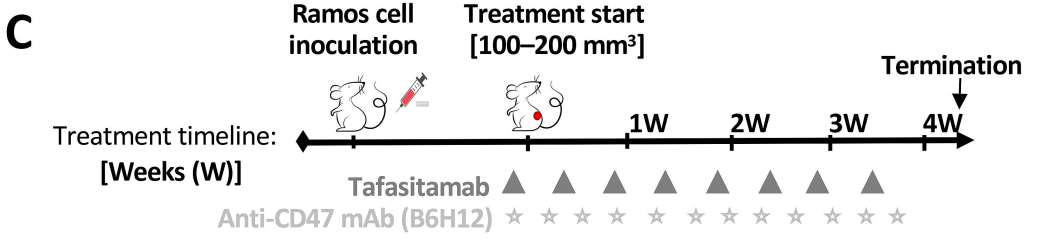
C
Ramos cell inoculation
Treatment start [100–200 mm³]
Termination
Treatment timeline:
[Weeks (W)]
1W
2W
3W
4W
Tafasitamab
Anti-CD47 mAb (B6H12)

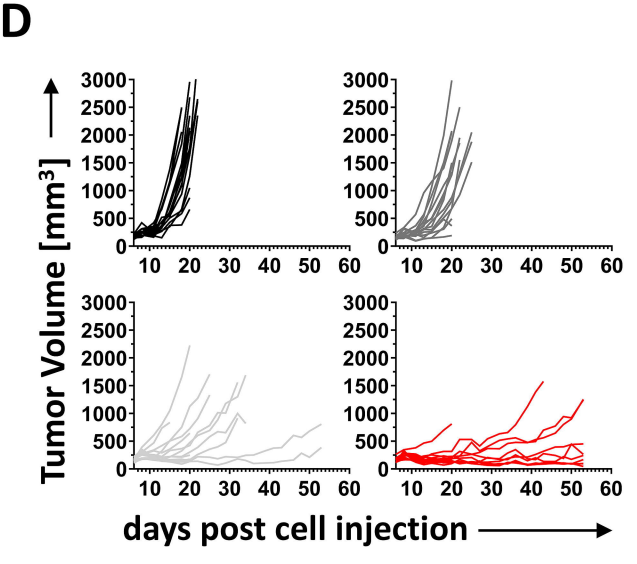
D
Tumor Volume [mm³]
days post cell injection

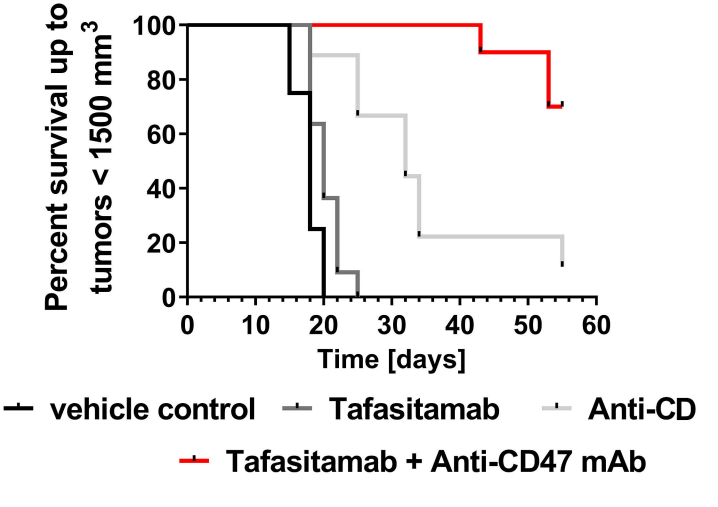
E
Percent survival up to tumors < 1500 mm³
Time [days]
vehicle control
Tafasitamab
Anti-CD
Tafasitamab + Anti-CD47 mAb

Blockade of the CD47/SIRPα checkpoint axis potentiates the macrophage-mediated anti-tumor efficacy of tafasitamab

Supplement

Materials and Methods

Cell-culture reagents

Cells were cultured in complete medium (referred to as R10), which comprised RPMI 1640 medium (Cat. #11875085, Biochrom, Berlin, Germany) supplemented with glutamine (2 mM; Cat. #G8540, Sigma), 10 mM HEPES (Cat. #P05-0110), 13 mM NaHCO3 (Cat. #P06-22100), 100 µg/ml streptomycin (Cat. #P06-11100P), 60 µg/ml penicillin (Cat. #P06-08100P) (all from Biochrom) and 10% Fetal Calf Serum (C.C.Pro, Charge Nr. C 591).

Cell lines

The DLBCL cell lines Toledo (CRL-2631) and HT (CRL-2260) were purchased from ATCC and U2946 (ACC 795) was purchased from the German Collection of Microorganisms and Cell Cultures (DSMZ, Braunschweig, Germany). Cell lines were used for no longer than 16 passages. All cell lines used in this study were monitored for mycoplasma contamination monthly using polymerase chain reaction (PCR) on all cell lines used in this study.

Antibodies and reagents

The following antibodies were used for immunofluorescence, flow cytometry or functional assays: CD19-APC (SJ25-C1, BD Pharmingen), CD19-Pe-Cy7 (SJ25C1, BD Pharmingen), CD19-BV421 (HIB19, BD Pharmingen), CD19-PE (FCM63, Merck/Milipore), CD19-PE (HIB19), CD19-PE (REA675, Miltenyi), CD68 (PG-M1, Dako Cytomation, Hamburg,

Germany), CD163 (10D6, Novocas-tra/Leica, Newcastle Upon Tyne, United Kingdom), CD163-PE (GHI/61, eBioscience, Frankfurt, Germany), CD163-BV421 (GHI/61, Biolegend), CD15-BV510 (W6D3, Biolegend), CD11b-FITC (M1/70.15.11.5, Miltenyi Biotec), CD11b-PeCy7 (ICRF44, BD Pharmingen), CD11b-APC (M1/70.15.11.5, Miltenyi Biotec), Annexin-V-APC (BD), 7-AAD (Sigma), CD47-FITC (B6H12, BD Pharmingen), CD47-PE (CC2C6, Biolegend), CD47-BV421 (B6H12, BD Pharmingen), SIRPα-PE (SE5A5, Biolegend), rabbit IgG F(ab')2 Fragment-488 conjugate, mouse IgG F(ab')2 Fragment Alexa-488, rabbit IgG F(ab')2 Fragment-674 conjugate, and mouse IgG F(ab')2 Fragment-647 conjugate (all from Cell Signaling Technology, Frankfurt, Germany). The Fc-silent antibody CD47-IgGo was generated as described previously[15]. Tafasitamab was provided by MorphoSys (MorphoSys AG, Planegg, Germany). The fluorescent probes were purchased from Essen Bioscience (Cytolight Rapid Green and IncuCyte® pHrodo® Red Cell Labeling Kit), from Sigma (DAPI, CFSE) and from eBioscience (VPD, Cell Proliferation Dye eFluor® 450; CPD, Cell Proliferation Dye eFluor® 670). 123count eBeads were purchased from eBioscience.

Lymph node biopsy and immunohistochemistry

Sections of 9 formalin-fixed and paraffin-embedded DLCBL or 7 reactive tonsil (benign controls) specimens were selected from the archive of the Institute of Pathology, University Hospital Erlangen, Germany. Sections were deparaffinized with xylol and rehydrated with graded ethanol. Antigen retrieval for all staining's was performed in a steam-cooker using a target retrieval solution pH 6 (TRS6; DAKO S1699) for 5 minutes at 120°C. Primary antibodies were incubated over night at room temperature. A triple-staining was performed with primary antibodies against CD68 (1:100, DAKO, monocloal, mouse, M0876), SIRPα (1:50, CellSignalling, monoclonal, rabbit; D6I3M) and CD206 (1:100, Novus, monoclonal, mouse, NBP2-52927) and fluorescence labelled secondary antibodies which were incubated for 30 minutes at room temperature (1:500, Alexa 488 labelled goat anti mouse IgG3, Dianova, 115-

545-209; 1:500, Alexa 555 labelled donkey anti rabbit, Lifetechnologies, A31572; 1:500 Alexa 647 labelled goat anti mouse IgG2b, Thermo Fischer A21242). Additionally, a double-staining for CD19 (1:50, Zytomed, monoclonal, mouse, MSK043-05) and CD47 (1:50; R&D, monoclonal, sheep, AF4670) was performed with fluorescence labelled secondary antibodies (1:500, Alexa 488 labelled donkey anti mouse, Lifetechnologies, A21202 and 1:500; Alexa 633 labelled donkey anti goat cross-reacting with sheep; Lifetechnologies, A21082). TrueVIEW autofluorescence Quenching Kit (Vector Labs; SP-8400) was applied for quenching in all staining's. Analyses of FFPE samples (9 DLBCL patients and 7 benign controls) were performed in a blinded fashion. After staining, the entire sections were scanned (Zeiss Axio Scan.Z1) and images were analyzed. Regions of Interest (ROIs) matching lymphoma cells/B-cells ($CD19^+$) or macrophages/LAMs ($CD68^+$) were segmented using Zeiss-software (ZEN 2.6) or the open-source software QuPath (https://qupath.github.io), and the mean fluorescence intensity (MFI) of CD47 or SIRPα was assessed for each ROI. The frequency of double-positive B cells ($CD19^+/CD47^+$) on the entire section was analysed using QuPath. Data from 25 lymphoma cells or macrophages from each donor were used for CD47/SIRPα expression levels. For this purpose, five image fields were selected per section and a total of more than 25 lymphoma cells ($CD19^+$) or macrophages ($CD68^+$) were analysed for their respective CD47 or SIRPα expression.

In vitro differentiation of human macrophages

PBMC were isolated by density gradient centrifugation of buffy coat preparations from the peripheral blood of healthy donors (Department of transfusion medicine, University Hospital Erlangen, Germany). Monocytes were isolated by plastic adherence and cultured in the presence of M-CSF (50 ng/ml, R&D) to generate macrophages. Macrophages were detached with EDTA (1mM, Sigma) after 6d of culture. Purity of generated macrophages was greater than 90% and minimally contaminated by CD3+ and CD19+ cells, determined via flow cytometry.

CPD, pHrodo or Cytolight green labelling of cells

Cells were stained in an incubator for 20 min in sterile PBS containing cell proliferation dye (5 µM, CPD) or Cytolight Rapid Green (0.5µM). Cell count was determined after washing the cells three times with R10 supplemented with heat inactivated FCS. To label with pHrodo dye, cells were washed twice with PBS and stained in with100 ng/mL IncuCyte® pHrodo® Red Cell Labeling Dye in an incubator for 1h. Cell count was determined after washing the cells once with IncuCyte® pHrodo® Wash buffer.

CRISPR Cas9

The CRISPR/Cas9 system was used to generate CD47-knockout and CD47-overexpressing Toledo cells. All necessary reagents were purchased from Horizon Discovery, as follows: Dharmacon, Inc. Edit-R™ Inducible Lentiviral Particles hEF1α-Blast-Cas9 (VCAS11227), Dharmacon, Inc. Edit-R™ CRISPRa Lentiviral Particles hCMV-Blast-dCas9-VPR (VCAS11918), Edit-R predesigned lentiviral sgRNA, CD47 human (CD47-Plasmid: GSGH11838-247009754). Target cells were infected with lentivirus particles encoding the Cas9 sequences for at least 24 hours, and subsequently selected with blasticidin (7.5 µg/mL 2 days, 10 µg/mL 3 days). Cells were cultivated for 7 days after removal of blasticidin and single cells were sorted in cell culture plates. Clones for further transduction were selected based on Cas9 expression determined via Western Blot. The CD47-plasmid was transfected with the packing plasmids into 293T cells to generate lentiviruses. Virus containing supernatant was collected 48–72 hours after transfection. To achieve infection, target cells were incubated with lentivirus particles for 48 hours and subsequently selected with puromycin (0.5-1 µg/mL), 48 hours after removal of the virus. The following sgRNA target sequence was used: Human CD47: TTGCTGGGCTCGGCGTGCTG (Exon 1).

Bioinformatical analysis

We searched the gene expression omnibus (GEO) for public transcriptomics data that would elucidate fundamental concepts of our hypothesis concerning DLBCL, the levels of CD47 and SIRPA. Accordingly, we found the study GSE178965 which profiled DLBCL patients and provided diseases status and outcomes. Hence the study presents an ideal fit for our investigation. Subsequently, we downloaded the raw count matrix provided on GEO and performed bioinformatic analysis to gauge possible trends in the expression of the genes. First, raw counts were fed into DESeq2 for differential expression analysis. Subsequent results were investigated of SIRPA or CD47 where both did not show significant differential expression. We further investigated however if there were trends observable over the patient cohort. Since primary patient data is usually marred with heterogeneity, we first performed outlier depletion by calculating the 25th and 75th percentile of expression measured by DESeq2's normalized and setting the upper and lower bound to 1.5 times the interquartile above or below the 25th or 75th percentile respectively. The R code for the analysis can be found under https://github.com/liscruk/cd47_analysis.

Incucyte®-based phagocytosis assay

Lymphoma cells were labeled with IncuCyte® pHrodo® Red Cell Labeling Kit and co-cultured with macrophages (E:T=5:1) in a 96-well flat bottom plate in the presence or absence of tafasitamab (1µg/ml) and/or anti-CD47 antibody (B6H12, 1µg/ml). The plate was placed in Incucyte® S3 Live Cell Imaging Microscope and measured every 15-30 minutes. Recorded images were later analyzed using Incucyte® 2022A software. Phagocytosis was determined by measuring the Total integrated intensity [RCUxµm²/image] of red fluorescent signal.

In vivo experiments

Orthotopic tumor model: 1×10^6 Ramos cells were injected into the tail veins of *C.B-17 SCID* mice on study day 0. Two days after cell inoculation, animals were randomized into four treatment groups of 15, based on body weight. On study day 5, treatment with vehicle control (PBS), tafasitamab (3 mg/kg), or anti-CD47 antibody (clone B6H12, BE0019-1, BioXCell; 4 mg/kg) commenced in mono- or a combination regimen. Tafasitamab was administered via an intravenous injection (i.v.), twice a week and anti-CD47 antibody by intraperitoneal injection (i.p.) three times per week for up to three weeks. Treatment volume was calculated and adjusted based on the animal's individual body weight before each dose administration. Clinical signs and body weight loss were monitored until individual ethical endpoint or study termination on day 99 after cell inoculation.

Flank tumor model: $1x10^7$ Ramos cells mixed with 50% (v/v) matrigel (ref. 356237, Corning) were injected into the right flank of *NOD/SCID (NOD.CB17-Prkdcscid/J)* mice. On study day 6, when mean tumor volume reached 100 - 200 mm^3, animals were randomized and treatment with vehicle, tafasitamab (10 mg/kg/dose) or anti-CD47 antibody (clone B6H12, BE0019-1, BioXCell, 4 mg/kg/dose) either alone or in combination commenced. Tafasitamab and the anti-CD47 antibody were administered i.p. two and three times weekly, respectively, for four weeks. Clinical signs and body weight loss were monitored until individual ethical endpoint or study termination on day 55 after cell inoculation. Tumor size was measured twice weekly and tumor volume was calculated using the following formula: $width^2$ x length/2. Kaplan Meier curves depict the time until tumor size reached a volume of 1500 mm^3.

Animal procedures and experimentation were authorized by the French Comité National de Réflexion Ethique sur l'Expérimentation Animale and the Pennsylvania State College of Medicine Institutional Animal Care and Use Committee.

Supplemental Figure 1

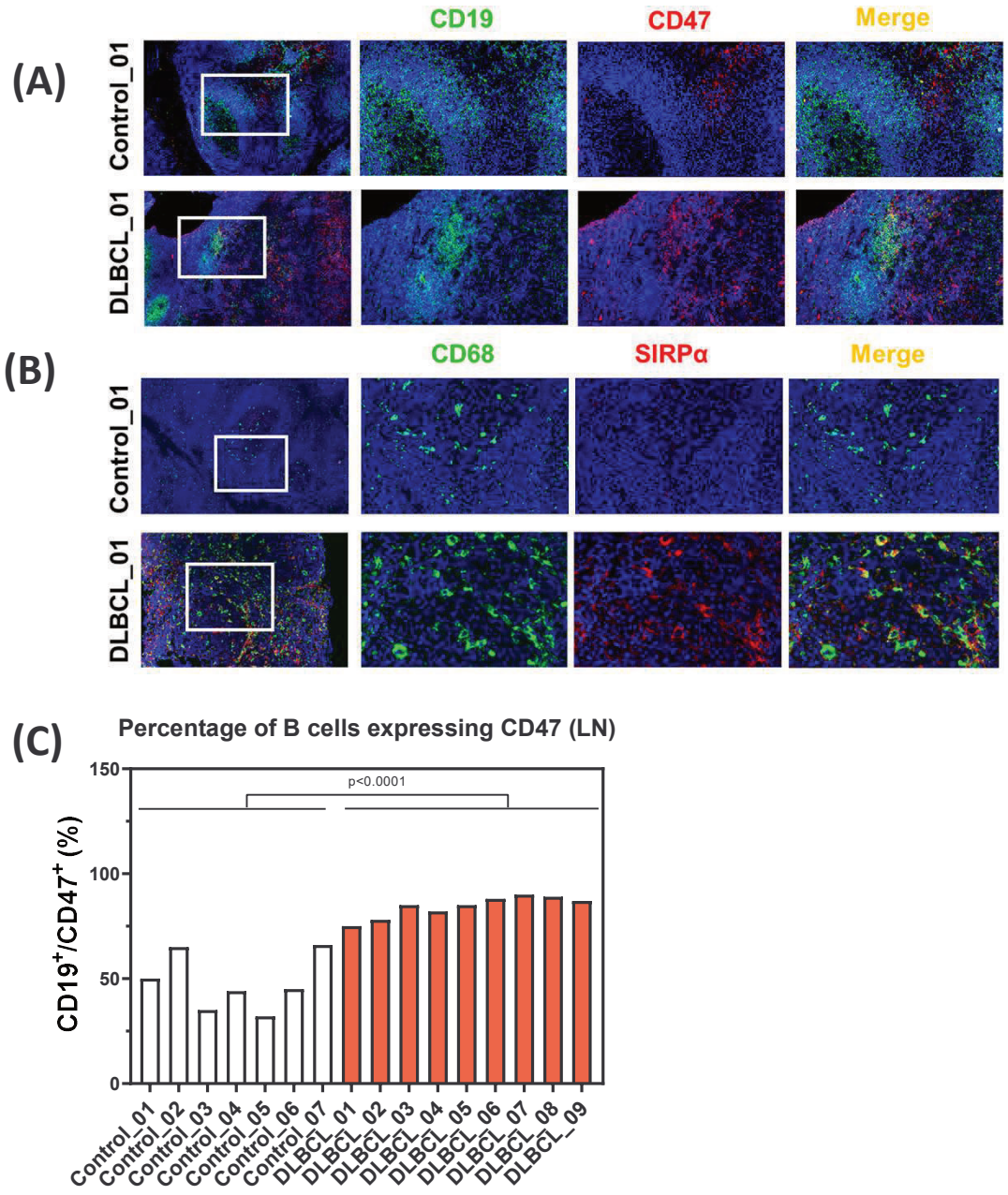

Supplementary Figure 1

(**A**) Expression of CD47 (red) on B-cells (CD19, green) (upper panel) and (**B**) SIRPα (red) on macrophages (CD68, green) (lower panel) was quantified using confocal microscopy on tonsils as benign controls (n=7) or DLBCL specimens (n=9). The microscopy images show representative sections of all experiments. (**C**) The percentage of CD47 expressing B-cells was quantified using confocal microscopy on tonsils as benign controls (white bars) (n=7) or DLBCL specimens (red bars) (n=9). QuPath (https://qupath.github.io) was used to segments the cells and calculate the percentage of CD47-expressing $CD19^+$ lymphoma/B cells on the whole sections. Each bar represents a tested donor. Nonparametric Mann-Whitney U-test was performed.

Supplemental Figure 2

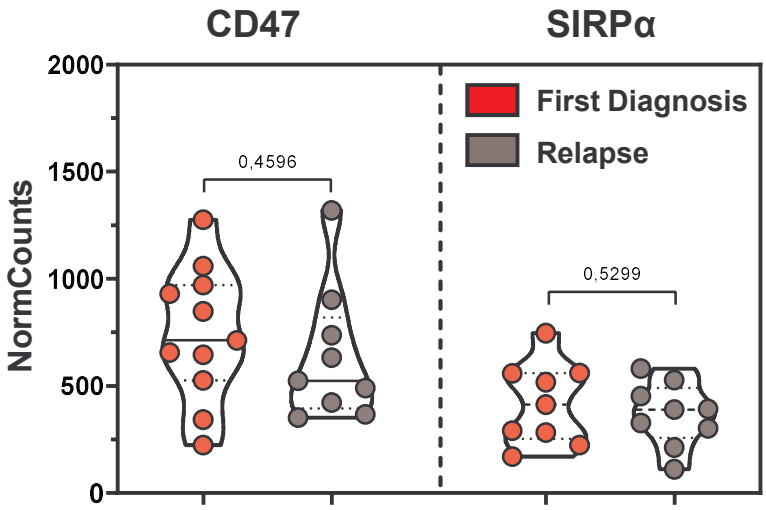

Supplementary Figure 2

Expression of CD47 and SIRPα in lymph node biopsies of newly diagnosed (red dots, n=11) or relapsed (grey dots, n=9) DLBCL patients from publicly available transcriptomics data are shown as normalized counts. Normalized counts were extracted after running DESeq2. Shown are the expression values in the analyzed samples after removal of strong outliers, defined by removal of all samples lying outside the 1.5-fold interquartile range in both directions. Two tailed paired Students t test was performed.

Supplemental Figure 3

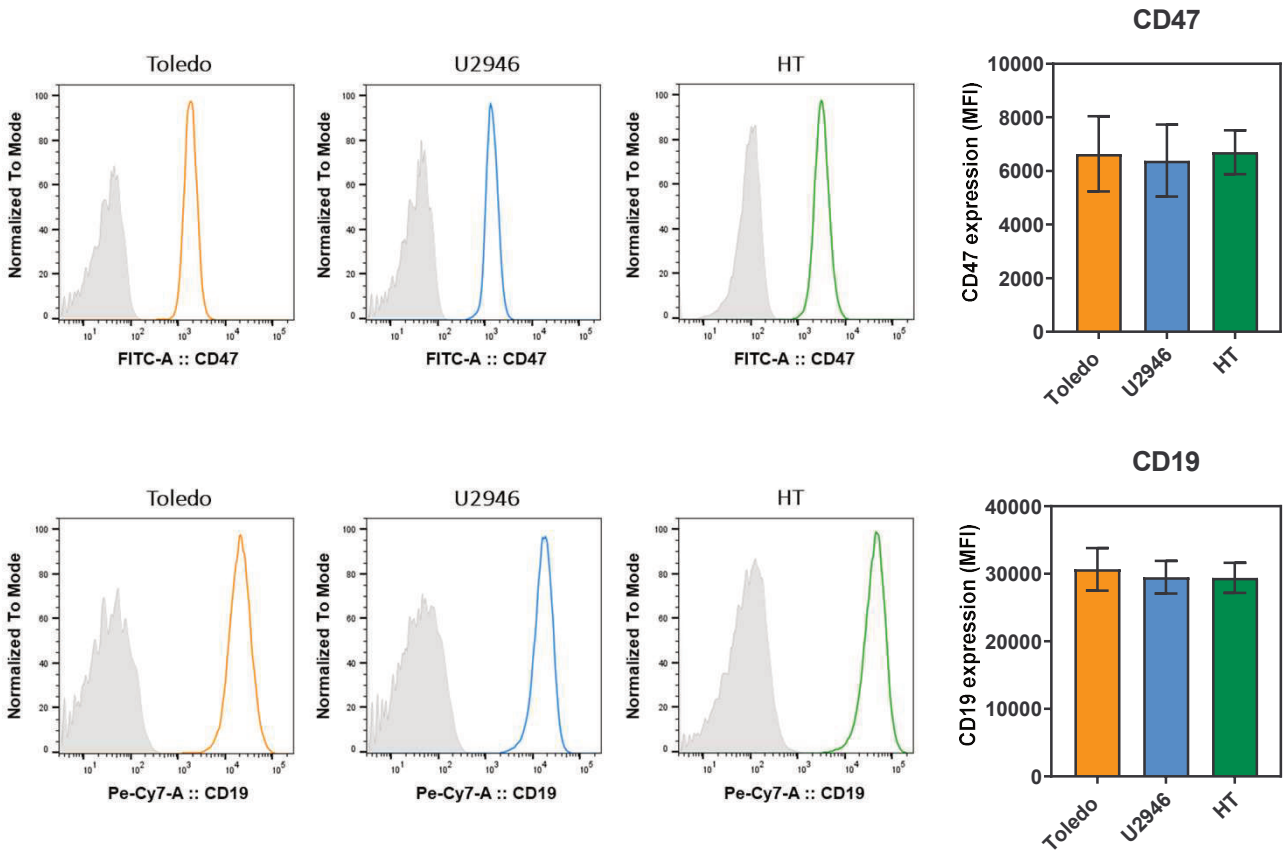

Supplementary Figure 3

CD47 (upper panel) and CD19 (lower panel) expression in DLBCL cell lines. Cells (Toledo, orange; U2946, blue and HT, green) were stained for CD47 and CD19 and surface expression was measured by flow cytometry. Grey histogram represents the isotype control. Surface expression was calculated as Mean Fluorescence Intensity (MFI) of cells stained with anti-CD19 or anti-CD47 antibodies. The graph shows the average result of four independent experiments. Error bars show SEM.

Supplemental Figure 4

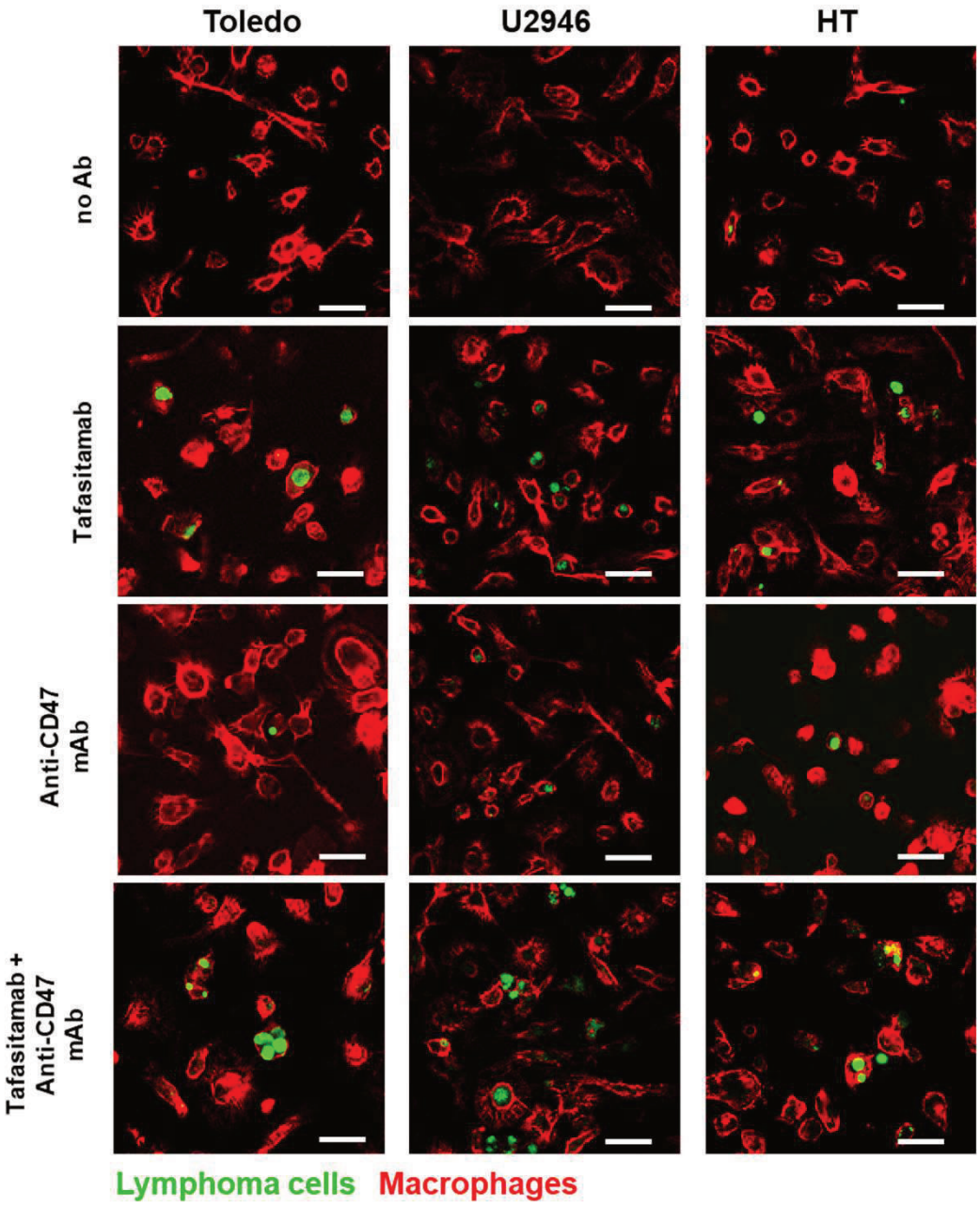

Supplementary Figure 4

Immunofluorescence of *in vitro* differentiated macrophages (red) co-cultivated with indicated cell lines (Toledo, U2946, HT) (green) and tafasitamab +/- anti CD47-mAb (1µg/ml) for three hours to detect phagocytosis. Images were taken after washing steps, removing non-adherent and/or non-phagocytosed cells. The microscopy images show representative sections of five performed experiments. Scale bar: 20µm.

Supplemental Figure 5

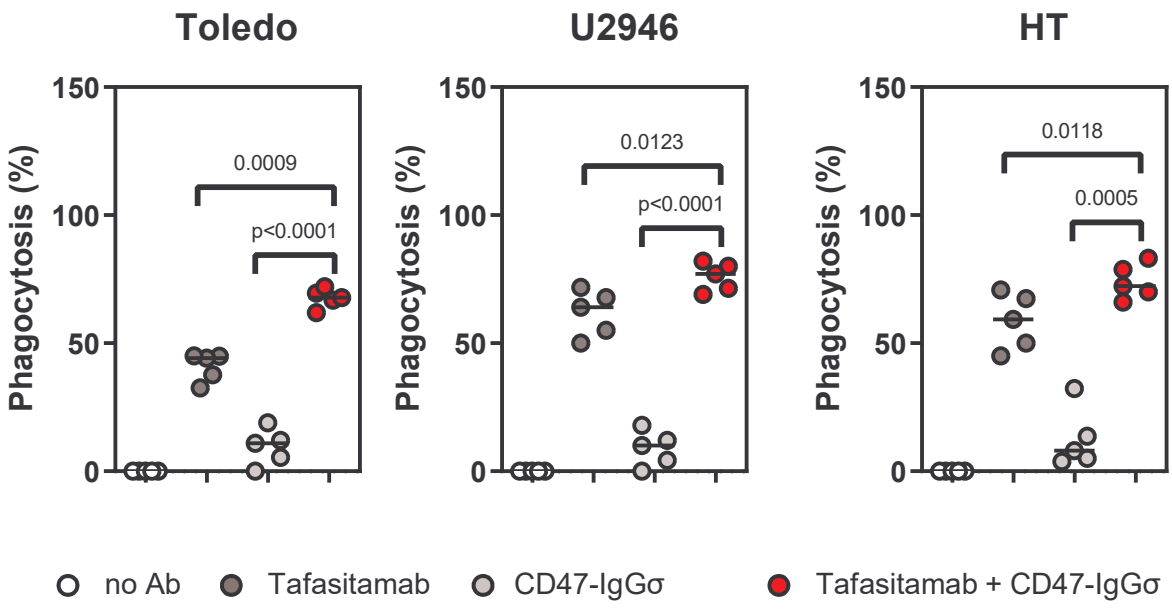

Supplementary Figure 5

Quantification of phagocytosis by Incucyte microscopy. Macrophages were co-incubated with fluorescently labeled lymphoma cells (as indicated) in the absence (white circles) or presence of tafasitamab (dark grey circles) or anti-CD47 (CD47-IgGσ, light grey circles) or a combination of both (red circles). After 3 hours, phagocytosis was analyzed and quantified by Incucyte microscopy and Incucyte® 2022A software. The graphs show the result of five independent experiments. Lines show the mean value. Two tailed paired Students t test was performed.

Supplemental Figure 6

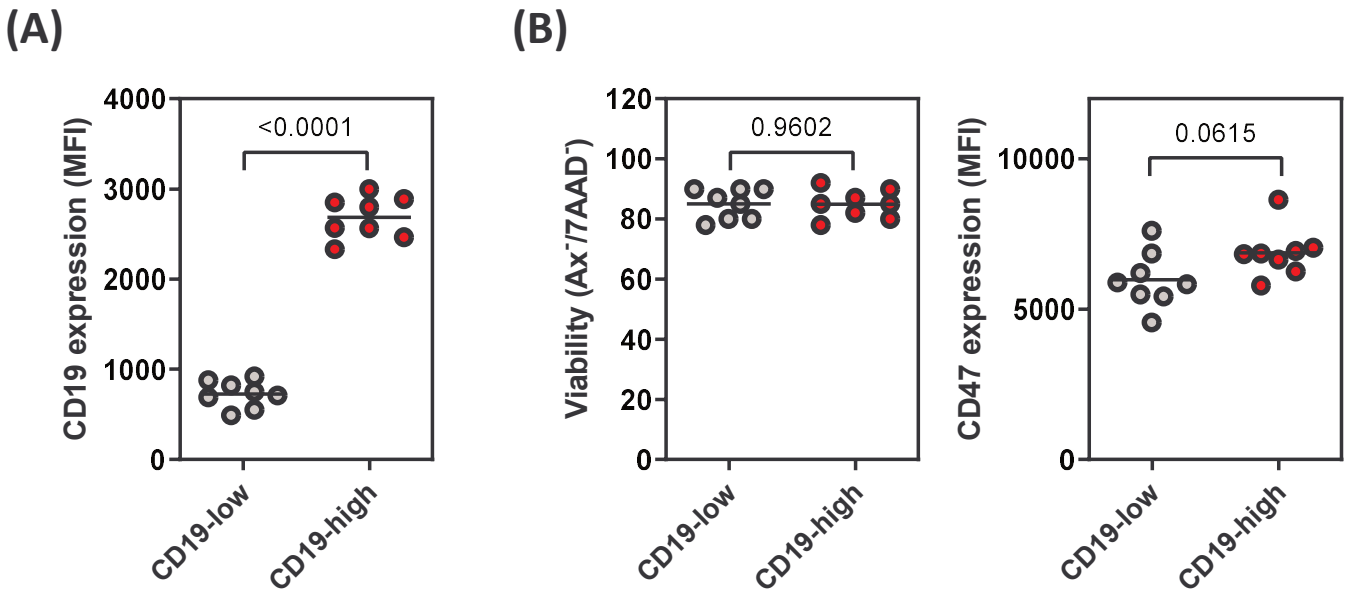

Supplementary Figure 6

Phenotype of sorted Toledo cells. The cell line Toledo was stained with an anti-CD19 antibody and separated in CD19 low expressing (CD19-low, grey circles) or CD19 high expressing (CD19-high, red circles) cells by flow cytometry. Isolated cells were subsequently analyzed for their (**A**) CD19 surface expression or for their (**B**) viability and CD47 expression. Surface expression was calculated as Mean Fluorescence Intensity (MFI) of cells stained with anti-CD19 or anti-CD47 antibodies. Viability of isolated cells was measured by Annexin-V and 7-AAD by flow cytometry. The graphs shows the average result of eight independent experiments. Lines show the average value. Two tailed paired Students t test was performed.

Supplemental Figure 7

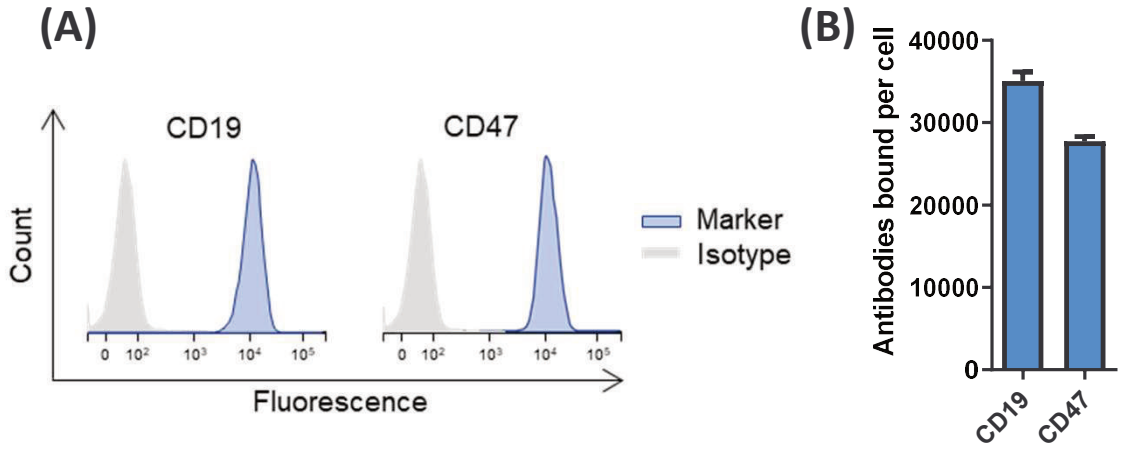

Supplementary Figure 7

Flow cytometric analysis of CD19 and CD47 expression on Ramos cells. (**A**) Ramos cells were stained for CD47 and CD19 (blue histograms) or isotype control (grey histograms) and surface expression was measured by flow cytometry. (**B**) Surface expression of CD19 and CD47 receptors was analyzed using the Quantibrite system (BD Biosciences), according to manufacturer's instructions. Mean fluorescence intensity (MFI) values were measured upon staining with PE-labeled anti-CD19 or anti-CD47 antibodies, and the MFI values of reference beads were used to correlate MFI to the number of antibodies bound per cell via linear regression. The graph shows the average result of three independent experiments. Error bars show SEM.

Supplemental Table 1: Patients' characteristics (FFPE)					
Case No.	Sex [m/f]	Age [years]	Cell-of-origin subtype Hans criteria	IPI risk group	Figure
1	m	53	GCB	Low-intermediate	1A, 1B, Suppl.1
2	m	77	GCB	high-intermediate	1A, 1B, Suppl.1
3	f	68	non-GCB	high	1A, 1B, Suppl.1
4	m	75	non-GCB	Low-intermediate	1A, 1B, Suppl.1
5	f	81	non-GCB	high	1A, 1B, Suppl.1
6	f	59	non-GCB	Low-intermediate	1A, 1B, Suppl.1
7	f	80	GCB	Unknown	1A, 1B, Suppl.1
8	m	87	non-GCB (not clear)	Low-intermediate	1A, 1B, Suppl.1
9	f	81	non-GCB	Low-intermediate	1A, 1B, Suppl.1

Supplemental Table 2: Patients' characteristics (viable cell data)				
Case No.	Sex [m/f]	Age [years]	Cell-of-origin subtype Hans criteria	Figure
1	f	47	non-GCB	1C, 1D, 4C
2	f	57	non-GCB	1C, 1D, 4C
3	f	61	non-GCB	1C, 1D, 4C
4	m	48	GCB	1C, 1D, 4C
5	m	53	non-GCB	1C, 1D, 4C
6	f	28	non-GCB	1C, 1D, 4C
7	m	67	non-GCB	4C
8	m	75	GCB	1C, 1D, 4C
9	m	54	non-GCB	4C
10	m	61	non-GCB	4C
11	f	75	non-GCB	4C
12	m	39	non-GCB	4C
13	f	62	non-GCB	4C
14	m	65	GCB	1C, 1D, 4C
15	m	60	GCB	1C, 1D, 4C
16	m	79	non-GCB	4C
17	f	63	GCB	4C

FFPE: formalin-fixed paraffin-embedded; m: male; f: female; GCB: germinal center B-cell like